

LAPPEENRANTA UNIVERSITY OF TECHNOLOGY
LUT School of Energy Systems
LUT Mechanical Engineering

Kshitiz Rai

DESIGN OF SOFT ACTUATOR BASED HAND-EXOSKELETON FOR
REHABILITATION AND ACTIVITIES OF DAILY LIVING

Supervisor & Examiner: Adjunct Professor Huapeng Wu
Ph.D. Ming Li

ABSTRACT

Lappeenranta University of Technology
LUT School of Energy Systems
LUT Mechanical Engineering

Kshitiz Rai

Design of soft actuator based hand-exoskeleton for rehabilitation and activities of daily living

Master's thesis

2018

55 pages, 34 figures, 6 table

Supervisor & Examiners: Adjunct Professor Huapeng Wu
Ph.D. Ming Li

Keywords: EEG, exoskeleton, actuators, biomechanics, rehabilitation, ADL

As a result of aging, hand strength reduces significantly. This leads to insufficient grab and pinch strength needed to perform daily activities such as preparing tea and holding cups. Subsequently, personal assistant for elderly are hired. On the other hand, the post stroke survivors need hand rehabilitation to restore back the strength loss due to paralysis. In both cases, the restoration of physical strength is both essential and beneficial.

This thesis project investigates the possibility of designing a novel Hand Exoskeleton (HE) suitable for both post stroke rehabilitation and Activities of Daily Living (ADL) purposes. Based on the literature reviews and analysis, a pneumatic actuation system is chosen for developing a soft rotary artificial muscle that is capable of driving the fingers into extension and flexion motion. For this, a silicone rubber of 30 shore durometer is additive manufactured to form a soft rotary actuator. The actuators are assembled with the 3D printed exoskeleton frame to form a complete HE system. The performance results of the system is then presented. With the main aim of increasing the strength to weight ratio, the research has shown the potential to achieve the target. Furthermore, the research is successful in achieving other objectives too.

ACKNOWLEDGEMENTS

I would like to thank my supervisor Adjunct Professor Huapeng Wu for providing me an opportunity to work on the Brain Controlled Ankle-Foot/Hand Orthosis project and do my thesis. His support and guidance have been invaluable for successful completion of my thesis work. I would like to thank all the members of the project and their support during the project.

I would like to express my sincere gratitude to my family, my mother, father and sister for their unconditional love and support throughout my years of study. Also, many thanks to my wonderful friends, Prakash, Dinesh, Shiva, and Devika for their support and suggestions during my thesis.

Finally, to everyone who have been directly or indirectly involved in making this thesis successful.

Kshitiz Rai

Lappeenranta 30.12.2017

TABLE OF CONTENTS

LIST OF ABBREVIATIONS	5
1 INTRODUCTION	6
1.1 Research Background	6
1.2 Objectives and Research Questions	7
1.3 Research Methods	8
1.4 Overview of BCAFO project	9
1.5 Structure of the Thesis	12
2 OVERVIEW OF HAND-EXOSKELETON	13
2.1 Characteristics of the Hand Exoskeleton	13
2.2 Review of Literatures	16
2.3 Effect of Human Biomechanics	20
2.3.1 Anatomy of the Human Hand	20
2.3.2 Mathematical Modeling of Human Hand Finger	24
3 THE DESIGN	28
3.1 Materials	28
3.2 Hand Exoskeleton Frame Structure	30
3.3 Actuator Structure	32
3.4 The Control system	36
4 RESULTS AND ANALYSIS	38
4.1 Performance of HE frame structure	38
4.2 Performance of Actuators	42
5 CONCLUSION	47
LIST OF REFERENCES	49
APPENDIX	
Appendix I: Total Deformation of the DIP Joint Actuator (Cross Sectional View)	
Appendix II: Equivalent Elastic Strain of the DIP Joint Actuator (Cross Sectional View)	

LIST OF ABBREVIATIONS

3D	Three Dimension/al
ADL	Activities of Daily Living
BCAFO	Brain Controlled Ankle-Foot/Hand Orthosis
CAD	Computer Aided Design
CMC	Carpometacarpal
DC	Direct Current
DI	dorsal interossei
DIP	Distal Interphalangeal
DOF	Degrees of Freedom
EEG	Electroencephalography
FEA	Finite Element Method
HE	Hand Exoskeleton
IP	Interphalangeal
MCP	Metacarpal Interphalangeal
NiTi	Nickel Titanium
PI	palmar interossei
PIP	Proximal Interphalangeal
ROM	Range of Motion
SMA	Shape Memory Alloy
WHO	World Health Organization

1 INTRODUCTION

This is an introduction to the Master's thesis "Design of soft actuator based hand-exoskeleton for rehabilitation and activities of daily living", as a part of Brain-controlled Ankle-Foot/Hand Orthosis (BCAFO) project supported by Academy of Finland. This chapter presents the research background, objectives and questions, an overview of the BCAFO project and structure of the thesis.

1.1 Research Background

The hand is one of the most important components in the human body to perform physical activities and maintaining daily life. From manipulating things to maintaining the physical balance, the hand has been key to human evolution and dominance. Although in all humans, the movement of hand-fingers is similar, the strength differs, primarily due to age, diseases and physical conditions (Carmeli et al. 2003). The hand movements may be semi or fully paralyzed due to various conditions such as post-stroke paralysis or other physical accidents. According to World Health Organization (WHO), the stroke patients in Europe (including EU and others) in 2000 were 1.1 million and is expected to rise to 1.5 million in the year 2025 (Truelsen et al. 2006). According to Thrift (Thrift et al. 2017), of all stroke survivors, nearly 80% suffer hemiparesis of upper arm affecting the hand motor predominantly. Even with the extensive rehabilitation methods after stroke, it is seen that the complete functional recovery is as low as 11.6%. The research pointed that the low recovery was linked to lack of voluntary motor control in the first 4 weeks of stroke. (Kwakkel et al. 2003).

Meanwhile, the cost associated with post-stroke rehabilitation significantly hinders the patients to actively participate in rehabilitation process in short or long term (Godwin et al. 2011). Along with human assistance, many post-stroke rehabilitation devices are in use (Heo et al. 2012). However, they are huge and expensive to own for personal use and thus are stationed at hospitals and rehabilitation centers. Thus, inadequate access to rehabilitation devices also aids to low recovery of post-stroke attack.

In another case, aging also significantly decrease the strength inhuman hand including grabbing, holding, pinching and ability to maintain a steady posture (Ranganathan et al. 2001, p 1483). Ageing is a natural phenomenon and thus, loss of physical strength due to it is an irreversible process. According to National Institutes of Health, the population of elderly (aged 65 years or over) is growing at a remarkable rate. Today, this age group holds 8.5% (617 million) of world's population and are expected to reach 17% by the year 2050 (1.6 billion). (National Institute of Health 2016). Majority of this huge population need assistance in maintaining daily activities including as simple task as, preparing coffee or eating food. The cost associated with hiring personal assistant or nurse is equally expensive. However, the use of assistive technology in elderly care is often less expensive than hiring a personal assistance (Miskelly, 2001).

In both cases of post-stroke paralysis and aging, the effect of hand dysfunction is troublesome. In order to address these cases, modern technology has developed various tools and techniques, which among them is a hand exoskeleton (HE). HE is an external structure that assists manipulation of human hand pursuing the hand trajectory. Usually, the HE is electrically or mechanically powered and play a vital role in assisting the life of impaired for rehabilitation and activities of daily living (ADL) purposes. However, the current HEs focus either one of the purposes. On the other hand, the rehabilitation HEs are bulky and expensive to own one. (Heo et al. 2012)

This thesis aims to develop a simple HE capable for both rehabilitation and ADL purposes. For a rehabilitation purpose, the system aids to smooth actuation of cyclic training of the affected hand. The HE is capable of delivering enough torque to maneuver the hand. On the other hand, for ADL purposes, the HE aids the hand by augmenting gripping and holding force in the hand. This significantly aid impaired for sustaining their daily livelihood in ease.

1.2 Objectives and Research Questions

As described earlier, post-stroke patients and elderly people are focused aspotential benefits of this research. Thus the primary objective of this thesis is to develop a simple and smooth actuation system capable of generating enough torque to achieve the basic functionality of assisting hand movements. However, while doing so the HE should always

follow the human hand biomechanics to ensure safety. In general, the main objectives of the research thesis are presented below.

- To develop a bi-directional HE capable of generating enough torque for rehabilitation and ADL purposes. This includes transmission of sufficient power for extension and flexion of the fingers for rehabilitation training and generating enough grab force for holding things such as cup and jug for ADLs purposes.
- To develop HE with high power to weight ratio. In the current scenario, the weight of HE has been a major issue with respect to the power. Thus, this thesis aims to develop lightweight HE with use of modern lightweight yet strong materials and transfer high torque.
- To ensure comfortability and safety of the HE. The HE is aimed to reduce extra weight and materials and ensure that it is comfortable to the users. It is equally important that is easy to put on or take off the HE. Similarly, this thesis is aimed to design a system that fulfills the maximum safety criteria, including the risk of fatigue failure and abnormal movement of the human hand biomechanics.
- To design a simple portable HE for everyday use. The existing HEs are usually complex mechanical, hydraulic or electrical systems and most of them are non-portable. This thesis aims to find a solution to design a straight forward HE which can be transferred as per desire.

Similarly, this thesis intends to answer the following research questions:

- How effective is the pneumatic actuation system in HE compared to others, e.g. hydraulic or electric? How about the accuracy?
- How does the system ensure the comfortability and safety with a reduction in weight?
- What effect does it have on the performance with the simple design of the HE?

1.3 Research Methods

This thesis is based on both qualitative and quantitative research approaches. For the qualitative approach, the challenges and advantages of the research are analyzed. In addition, the motivation and effect of the research to the target group is taken into consideration. On the other hand, for quantitative methods, the research focus significantly to increase the ‘strength to weight’ ratio based on previous researches to design a novel

HE. Mathematical modeling and technical calculations with laboratory tests are preferred to increase the validity of the quantitative approach. Figure 1 below provides an overview of the research methodology.

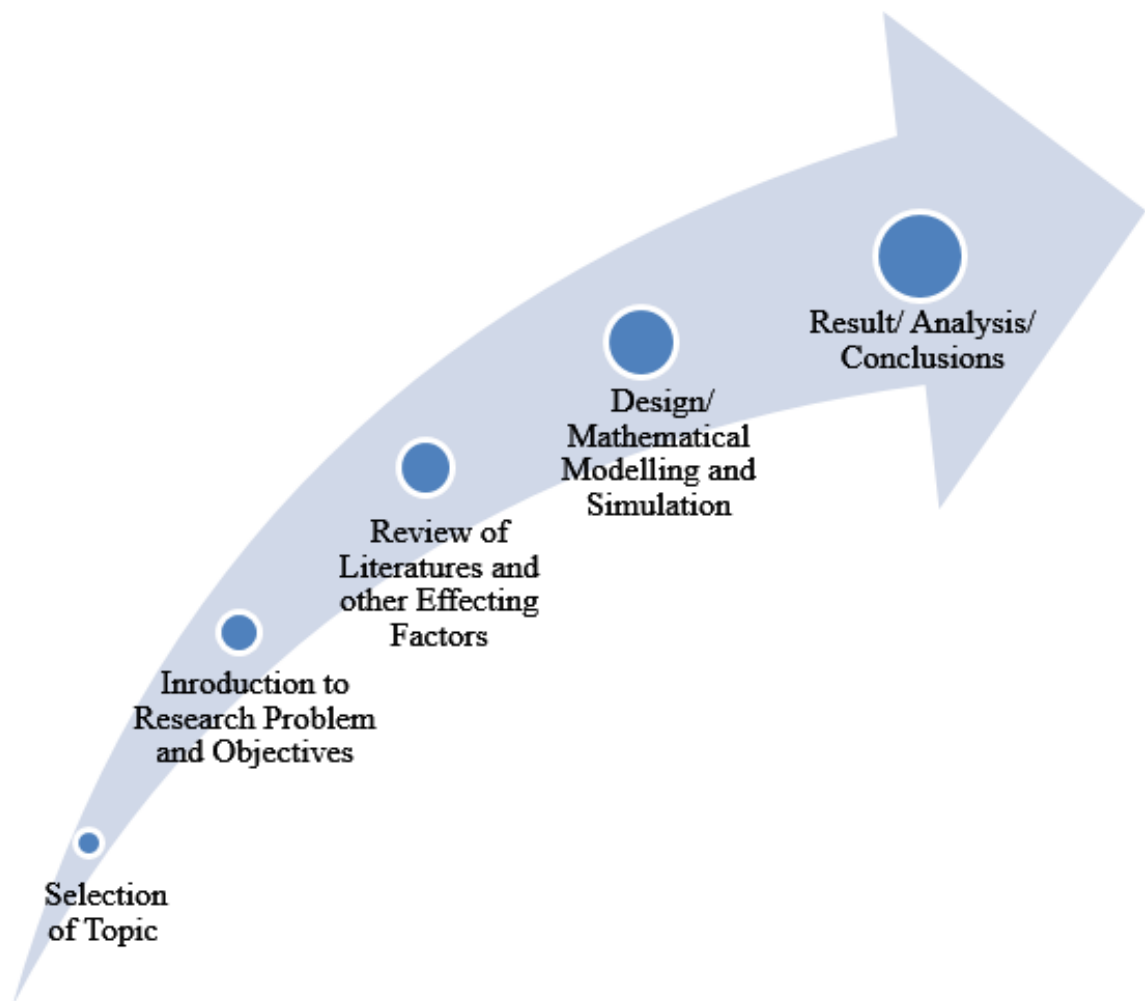


Figure 1. Overview of research methodology in the research

1.4 Overview of BCAFO project

This thesis is a part of BCAFO project accomplished at the Lappeenranta University of Technology. The project is aimed to control the HE via the power of thinking. Thus, in order to mechanically actuate the impaired hand, the BCAFO project utilizes EEG from the users. The minute electrical voltages in the brain are captured via EEG which are then processed. The thus simplified EEG signals are transferred to an electronic controller that controls the actuators, which is the primary component to mechanically flex or extend of the HE. The concept details can be illustrated by the Figure 2 below.

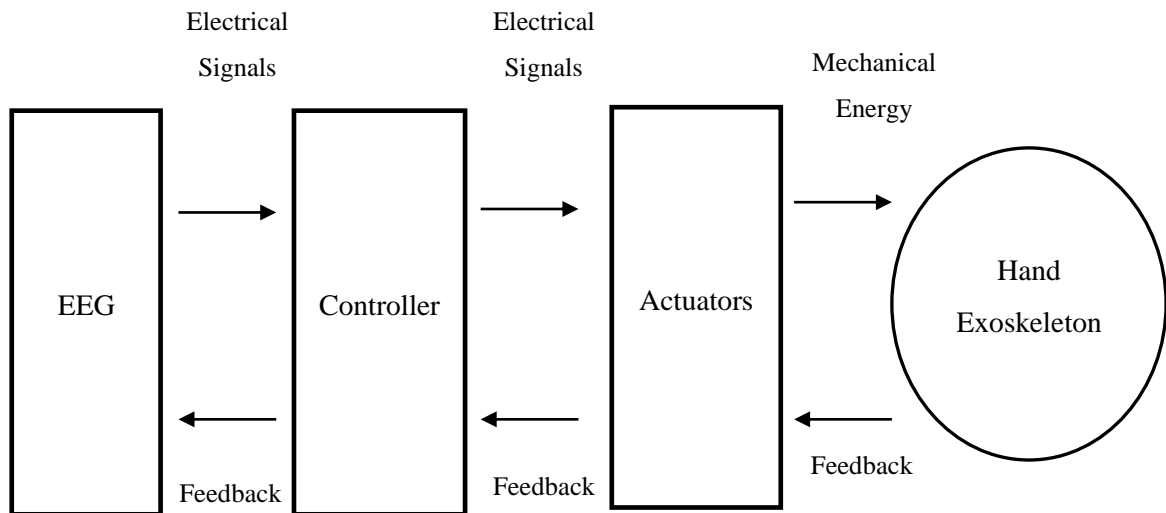
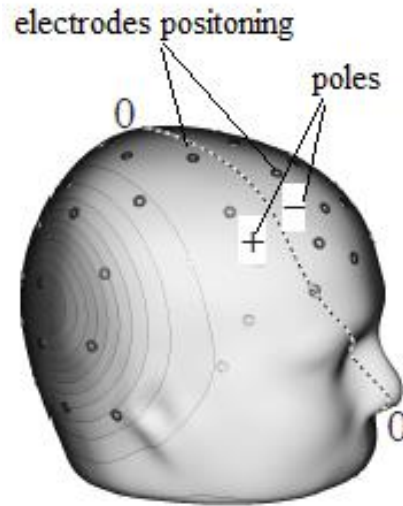


Figure 2. The basic concept of the BCAFO project as a part of this thesis research

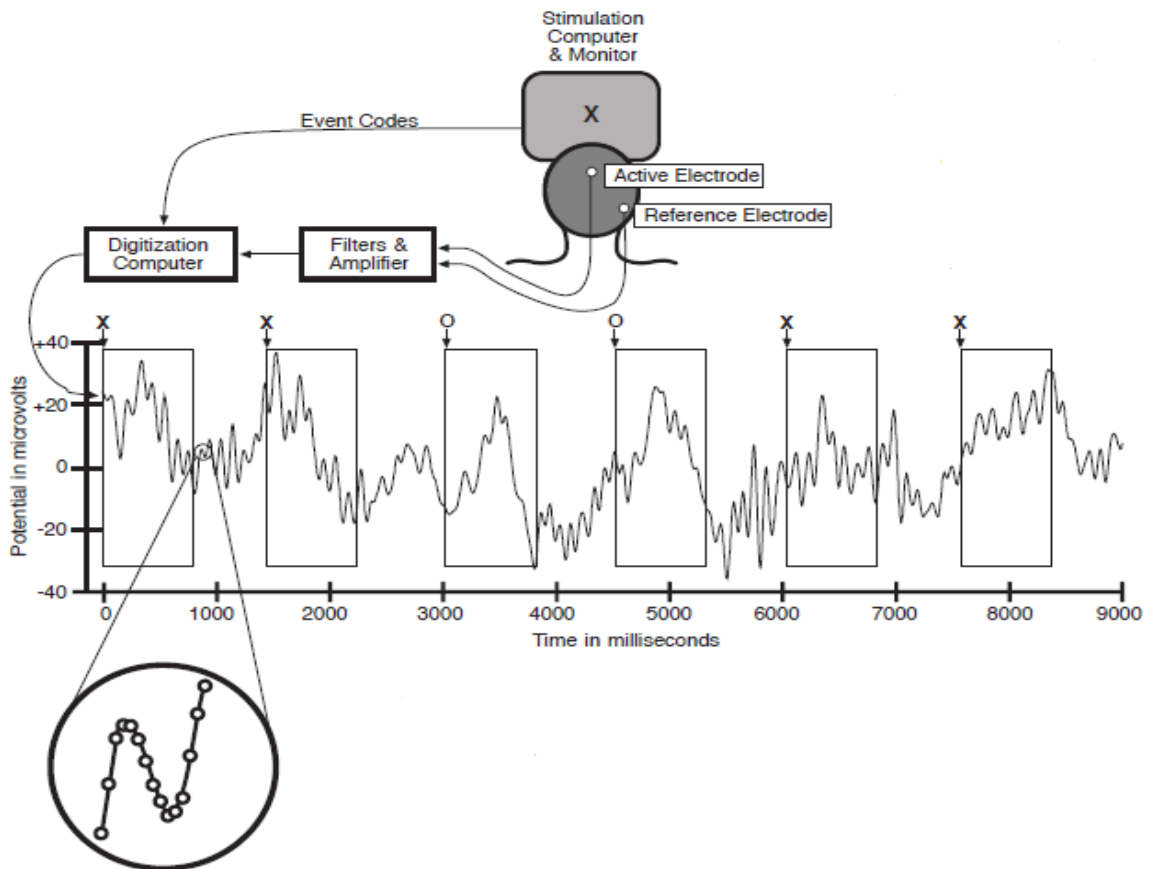
Synopsis of Electroencephalography

Electroencephalography (EEG) is a method of monitoring electrical activities in the cortical portion of the brain. It is an inexpensive and non-invasive process in which electrodes are positioned along the scalp (as shown in Figure 3(a)) to detect the voltage fluctuations arising inside the neurons in the brain (Niedermeyer et al. 2005). The voltage fluctuations detected by multiple electrodes are usually raw, noisy and highly attenuated due to various factors as sound interference, physical movement, light, length of the connected wires and so on. In order to utilize the raw EEG signals, they are imported to the simulation computer where they are amplified, filtered and finally plotted against the period of time (Figure 3(b)). The thus received signals provide important information for diagnostic applications and others.

Diagnostic application emphasis on two potential approaches, first the brain response to explicit sensory, motor and cognitive occurrence and second, the spectrum of ECG. The first approach examines the sudden variation in the signal to events as picking objects. The signal in this approach is time domain. On the other hand, the spectrum analyses the brain waves in EEG in a frequency domain. This is the main interest of the BCAFO project.



3 (a)



3 (b)

Figure 3.(a) is the electrodes distribution in a scalp in a dipole (positive and negative) configuration, (b) is the procedure used to measure EEG (Luck 2014).

While mainly used for diagnosis of various diseases and disorders as epilepsy and sleep disorder among others, now, researchers are investigating the potential to decode the human thinking via brain EEG. A successful interpretation of EEG leads to the control of the majority of human activities via thinking. One of the major beneficiary groups are the paralytic patients and elderly people. While having a semi or fully functionally brain, the EEG can be used to independently move paralytic/impaired hands via the use of the HE (Lee et al. 2017, p.21). This hugely aids them to move and work independently without the aid of another person.

1.5 Structure of the Thesis

This thesis report is divided into 5 key chapters. The first chapter is the introduction to the thesis. It explains the research background, objectives and research questions, and provide a short overview of the BCAFO project, associated with this research. The second chapter is a synopsis of the current HE. It introduces the characteristics of the HE, discusses the literature review and effect of human hand biomechanics. The third chapter contains the design of the HE. It includes the mechanical design of the HE and the actuator along with the control and supply system. The fourth chapter presents the results and discusses the interpretation of the achieved results. Finally, the fifth chapter presents the conclusion the thesis work.

2 OVERVIEW OF HAND-EXOSKELETON

2.1 Characteristics of the Hand Exoskeleton

The HE is a wearable external skeleton that supports the movement of the hand fingers. They are generally stimulated by electrical, pneumatic or hydraulic actuators and in recent times, also by Shape Memory Alloys (SMA) (Villoslada et al. 2016, p.91). The actuators help in flexion or extension or both of the fingers by the means of power transmission. According to Heo (2012, p.810), the HE can be classified into actuator type, sensing method, purpose and power transmission as shown in Figure 4 below.

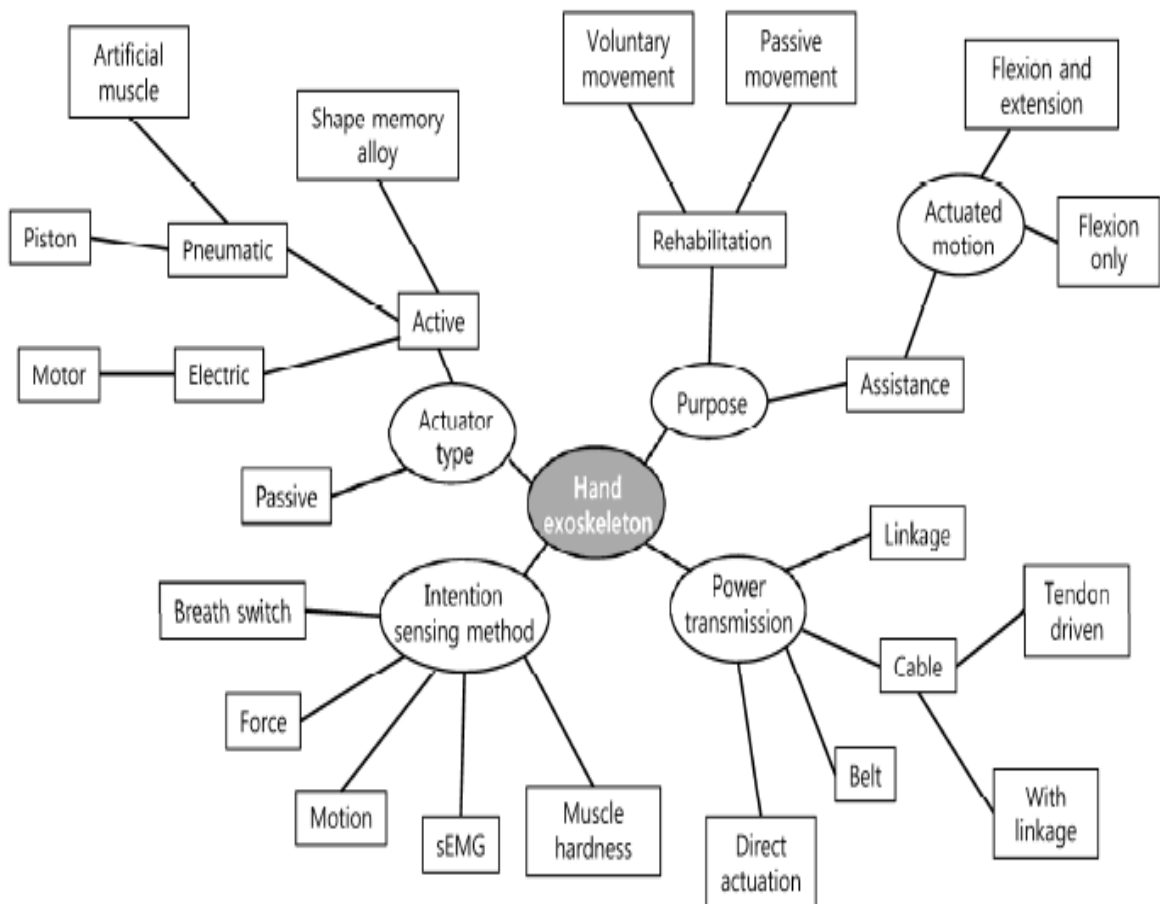
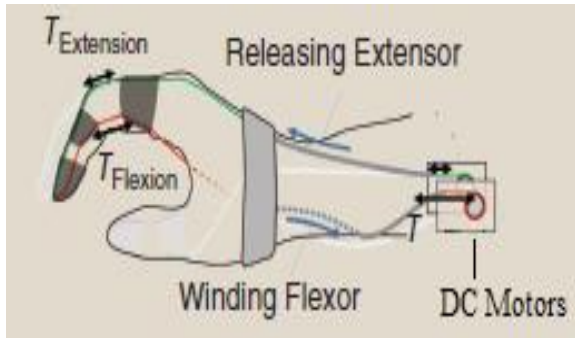


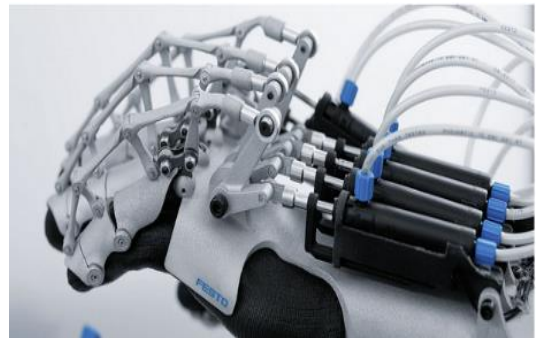
Figure 4. Classification of the HE according to various criteria (Heo et al. 2012. p.810)

Presently, there are three types of active actuators used for the HE actuation. These actuators primarily drive the HE via means of electric, pneumatic or SMA effect. Generally, electric DC motors, pneumatic piston, soft actuator/artificial muscle and Nickel-

Titanium (NiTi) alloys are mainly used for this purpose. The electric and pneumatic actuators provide better torque transmission than the SMAs in the HE functionality.



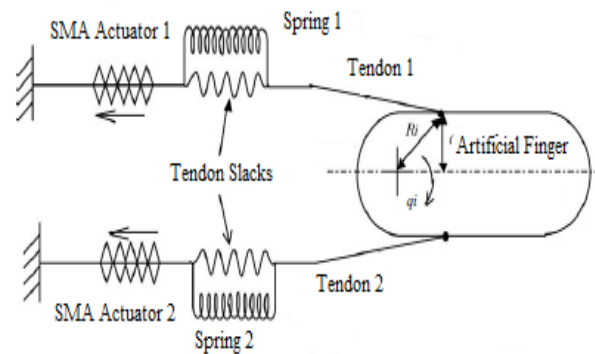
5(a) Electric Actuation of HE by DC motors



5(b) Pneumatic Piston Actuation Exo-Skeleton



5(c) Pneumatic Soft Actuation

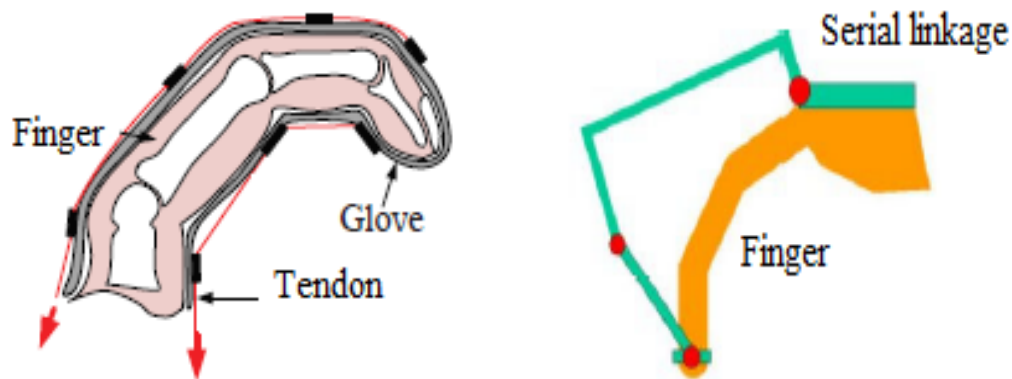


5(d) SMA driven actuation

Figure 5. (a) The electric-driven HE (In et al. 2015, p.99), (b) Pneumatic piston driven HE (Festo 2012), (c) The Soft actuator HE (Polygerinos et al. 2013, p. 1517), The SMA driven actuation for HE (Bundhoo et al. 2008, p. 8).

In order to actuate the HE, power transmission from the actuator to HE is necessary. There are many mechanisms to do so. One very common and widely used method is a cable driven mechanism. In this method, a tendon is used to transfer energy from the electrical actuator to the HE with or without the use of linkage. Similarly, belt and linkage are also used for power transmission. These methods are based on the remote location of actuators. On the other hand, power transmission can be made by direct actuation method. In this

method, an actuator is directly placed on the HE so that it does not require any means to transfer the power to the HE.



6 (a) A tendon driven HE

6 (b) A linkage driven HE

Figure 6. (a) A tendon driven HE (In et al. 2011). (b) A linkage driven HE (Stergiopoulos et al. 2003, p.84).

An accurate sensing of the HE movement is very important for controlling the device and ensuring the safety of the user. In order to do so, various methods and techniques are utilized. One of the widely used sensing methods is force feedback sensor. Usually, they are placed in a fingertip to determine the amount of force exerted by a grasp. This helps to avoid too high or too low forces that are capable of hurting the user's hand (Heo et al. 2012). However, the use of this sensor can block the haptic sensation of the user with the object. Similarly, motion sensing is very important to detect the bending angle of a finger. The human finger has a fixed trajectory and range. In order to stop the unnatural movement of the fingers, a motion sensing is used. The motion sensor feedbacks the finger trajectory to avoid any possible injuries that might be caused by the unnatural actuation of the HE.

Basically, two purposes, rehabilitation, and ADLs are served by the HE. For rehabilitation purpose, the HE generally follows a voluntary or a passive movement in a pre-defined trajectory of the flexion and extension. The fingers follow the same pattern throughout the session. This is typically designed to help the patient recover from hand paralysis by the means of training. On the other hand, the ADLs use actuated motion for 'flexion and

extension' or 'flexion only' as depending on the user to perform various household tasks as grabbing, holding or picking.

2.2 Review of Literatures

Over the decades, different HE have been developed for rehabilitation and ADLs purposes. They were designed with different approaches, such as; actuation type, size, power-weight ratio, portability, the comfort of wearing and so on, however, with a sole motive of assisting humans. These HE actuates either all or thumb-index-middle finger combination in a hand. Researches by Kargov (Kargov et al. 2004, p. 709) and Zheng (Zheng et al. 2011, p.4174) show that the humans typically use thumb-index-middle fingers for most of the time and work. These fingers generate the highest contact forces than any other fingers in combination. According to Iqbal (Iqbal et al. 2009, p.50), an exoskeleton having complete five fingers reduces the operational efficiency due to its increased weight and size and complexity of the system. Based on those facts, researchers as In (In et al, 2015) developed thumb-index-middle fingers actuated HE in 2015 and was successful in picking and grasping actions comfortably. They used electric motors to drive the HE.

Electric motors have been widely used actuators over the years. Electric motors are usually inexpensive, low weight and easy to control. Moreover, they generate required torque to drive the HE for opening and closing action. Researches made by Cempini (Cempini et al. 2013), Moromugi (Moromugi et al. 2009), Cortese (Cortese et al. 2015) and MA (MA et al. 2015), used electric motors to mechanically actuate the HE. Moromugi used tendons solely to transmit the torque. These tendons were guided into a specific guide to follow the path during its lifespan. As a result, the HE was lightweight, kinematic compatible, ensured proper torque transmission and was capable to achieve various hand gestures (as shown in figure 7). While others used tendons with linkages to transmit the torque from the directly placed actuators. As a result, HE was more rigid and forbid various gestures achieved by earlier research. Moreover, they were more complex and could only be used for rehabilitation purpose. However, all these HEs supported two way-movement (flexion and extension).

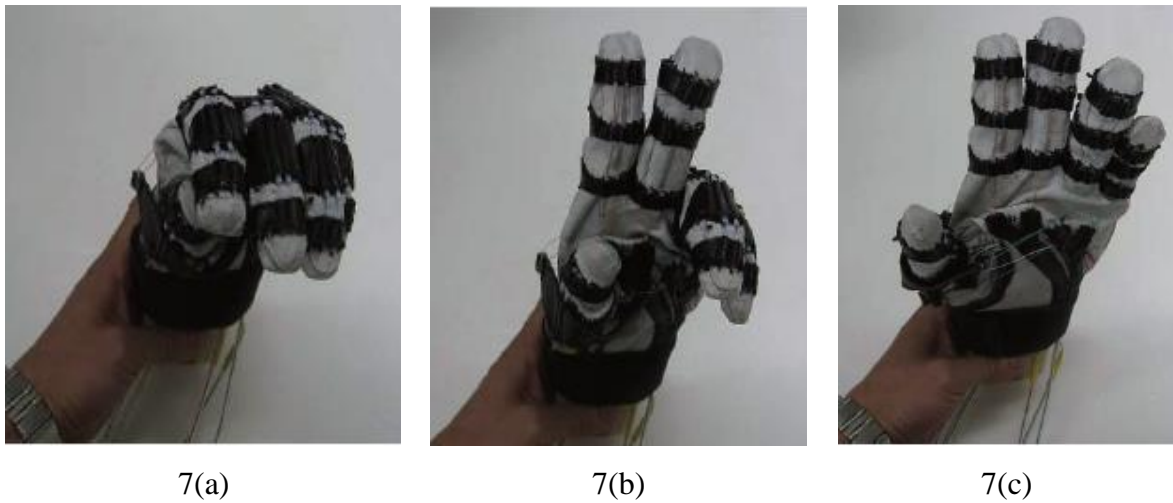


Figure 7. Different gestures achieved by the HE. (a) Pick rock (b) Pick scissors (c) Pick paper. (Moromugi et al. 2009.)

Similarly, Ueki (Ueki et al. 2012) and Zhang (Zhang et al. 2013) developed an electric motor powered HE but ended up with big size and complex systems. Thus they could only be used as a fixed station making them non-portable. These electric HE systems need continuous battery supply. Often low or empty battery result in stopping of a motor, subsequently locking the HE into a fixed gesture position causing discomfort for the users.

On the other hand, researchers have also used hydraulic and pneumatic systems to power the HE. The hydraulic system uses fluid pressure while pneumatic system uses compressed air to actuate the fingers. A research by Ryu (Ryu et al. 2008) used the micro hydraulic system to actuate the HE. The result was a lightweight, compact system with multiple degrees of freedom. Similarly, researches made by Polygerinos (Polygerinos et al, 2015) and Yap (Yap et al. 2015) showed that hydraulically actuated soft robotic glove with segmented elastomeric actuators with fiber reinforcements enable comfortable bending, twisting and extending motions. However, the research also concluded that fluid pressure causes oscillation in the system. Unlike this, on the other hand, pneumatic systems easily damp the oscillation. In 2010, Kotaro (Kotaro et al. 2010) and his team presented an oscillation-free pneumatic rubber muscle capable of generating enough torque to pick a 1kg weight. The similar pneumatic glove was developed by Lauri and his team in 2010 (Lauri et al. 2010). The glove assisted individual digit extension in hand opening and releasing phase of grasp. In 2013, Sun (Sun et al. 2013) developed a soft silicon rubber actuators

based on bending and rotary actions (as shown in figure 8). This design has opened a wide horizon of the possibility of use of low weight soft actuated HE.

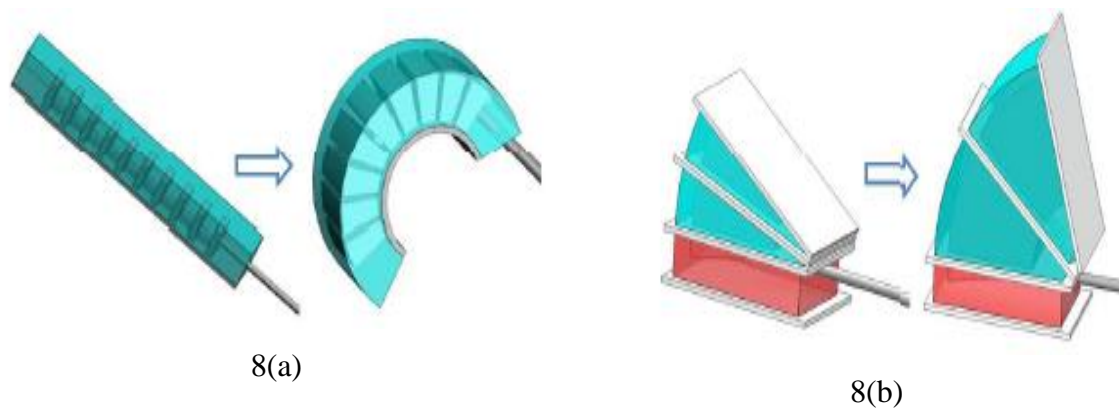


Figure 8. Demonstration of soft actuators under pressure. (a) Bending action of the soft pneumatic actuator (b) Rotating action of the soft pneumatic actuator. (Sun et al. 2013, p.4446)

There are, however, drawbacks associated with the hydraulic and pneumatic actuators in the HE. First, they are difficult to accurately control because of the non-linearity caused by the compressibility of the fluid/ air (Cladwell et al. 1995). Second, the system requires constant pressure supply. This makes the system noisy and difficult to move. This will overall affect the weight, stability, and range of exoskeleton. (Redlarksi et al. 2012).

In a situation like this, NiTi based SMA alloys can be useful actuators. They are low weight and can produce higher recovery force. However, in order to achieve the required stroke length for finger movement, the diameter and length of the SMA coil need to be long enough. (Yao et al. 2016). Furthermore, the SMA wires should be deformed at room temperature and activated in the acceptable temperature range for safe use. The Recent development of TiNi-based SMAs shows that the mechanical properties as transformation temperatures can be decreased and recovery strain can be increased to 8% with the addition of cobalt (Co) to TiNiNb alloy (Cai et al. 2006, p.299). On the other hand, it is seen that cyclic training of NiTi alloys lowers the transition temperature than the non-trained NiTi alloys (Lahoz et al. 2004, p. 135). These results have a huge benefit in the development of the HE. Likewise, a research by Lee (Lee et al. 2016), showed that SMAs generate high energy density to actuate fingers. However, they produce smaller pinch force of 5.7N in

comparison to commercial iLimb's (Bionics 2013) 17N and Bebionic's (Bebionic 2017) 15 N force powered by DC motor.

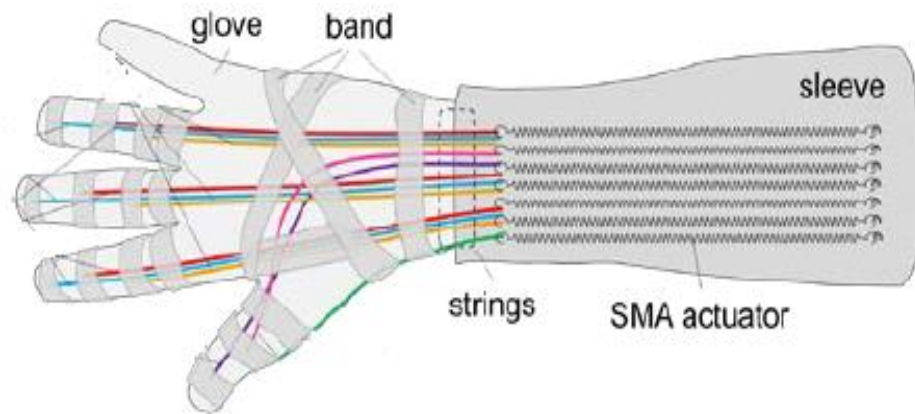


Figure 9. Representation of the SMA muscle glove (Yao et al. 2016)

Apart from these mechanisms, various others have been used in recent times. In the latest case, sliding springs have exposed a great potential to replace traditional cable driven mechanism for transmitting power. A research by Arata (Arata et al. 2013), used a three-layered sliding spring mechanism to power the HE. The HE was able to convert linear motion into three individual degrees of freedom in each finger along its digits. This technology proved to be compact and lightweight, and more importantly safe for individual use. In another case, a study has shown that a fiber actuator can be used for wearable applications (Hiraoka et al. 2016). The concept of fiber actuator is based on resistance heating, with the research gaining strain of 23% at 90°C. In order to utilize this technology safely, selection of right insulating materials is needed without hindering the user comfortability, which is one of the prime concern of this thesis.

In summary, there are many possibilities and limitations of using different methods and mechanisms as discussed above. For a comfortable wearable HE, soft actuators as, artificial muscle is found to be a better choice, as it undergoes soft actuation and has a low weight. Pneumatic actuation is found to be an ideal source of the power supply as it can be remotely placed, decreasing the effect of the weight on a hand. This thesis is closely based on the study of existing HEs and possibilities of future technologies to achieve the sole

target of increased mass-weight ratio and comfortability of the HE for the dual purpose of ADL and rehabilitation.

2.3 Effect of Human Biomechanics

Before developing the HE, it is very important to understand the mechanism of hand biomechanics. Hand biomechanics is a complex coordination of bones, joints, muscles, and ligaments working together to ensure the effective movement of the hand. As when the HE is worn, it closely follows the hand trajectory as their movement are coupled with each other. It cannot deviate from the arc of a hand, in order to ensure the safety of the user and provide an active maneuver. Particularly, to design a mechanically safe HE, it is important to study the of DOF and Range of Motion (ROM) of each joint. On the other hand, the hand movement is directly affected by the linked muscles and tissues. The intricacy nature of muscles and tissues adds complexity to the hand movement making them challenging to model mechanically. Thus, an efficient knowledge of hand anatomy is required for the proper design of the HE. (Heo et al. 2012)

2.3.1 Anatomy of the Human Hand

The human hand is highly articulated consisting roughly 30 DOF. Yet, it is also highly constrained having dependences among fingers and joints. (Lin et al. 2000, p. 121). The high articulation and constraints of the hand make it extremely difficult to model its movement. In addition, the irregular and complex biological joints and ligaments among bones and digits add further difficulty to truly map the kinematic model based on physiology. Thus, in order to learn the kinematics of pinching, gripping, and grasping of a human hand for the design of the HE, the knowledge of human hand is vital. The anatomy of the human hand can be presented in bones and joints, muscles, and ligaments.

The human hand consists of 27 bones arranged in a chain of carpals, metacarpals and, phalanges. The carpals are smaller bone segments forming a base of five single digits that are a poly-articulated chain of longer metacarpal and phalanx bone segments. These digits are thumb, index, middle, ring finger and little finger. Except thumb, all of the fingers are collection of one metacarpal and three phalanges. The thumb consists of only two phalanges (Grebenstein 2014). Two sets of carpal bones are attached to each other with

one linking the radius and ulna while other linking the metacarpals as shown in Figure 10(a), (b) and (c) below.

Each metacarpal is linked with carpals via carpometacarpal (CMC) joint. The CMC joint of each finger exhibit one DOF, except thumb that exhibits two DOF, flexion and extension, and abduction and adduction. (Heo et al. 2012, p. 808). The CMC joint of the four fingers is classified as a plain joint while the CMC joint of the thumb is classified as a semi saddle joint. The proximal phalanges (PP) are articulated to metacarpals via metacarpal phalanx (MCP) joints. These joints are classified as condyloid joints having 2 DOF, flexion and extension, and abduction and adduction. In MCP joint, the phalangeal base provides the suitable articulate surface for the metacarpal head (Figure 10(d)). Joints connecting PP and middle phalanges (MP) is called proximal interphalangeal (PIP) joint. On the other hand distal interphalangeal (DIP) joint is a joint between distal phalanges. The thumb lacks the DIP and PIP, but has only one interphalangeal (IP) joint. The PIP, DIP, and thumb IP joints are hinge joints and undergo one DOF.

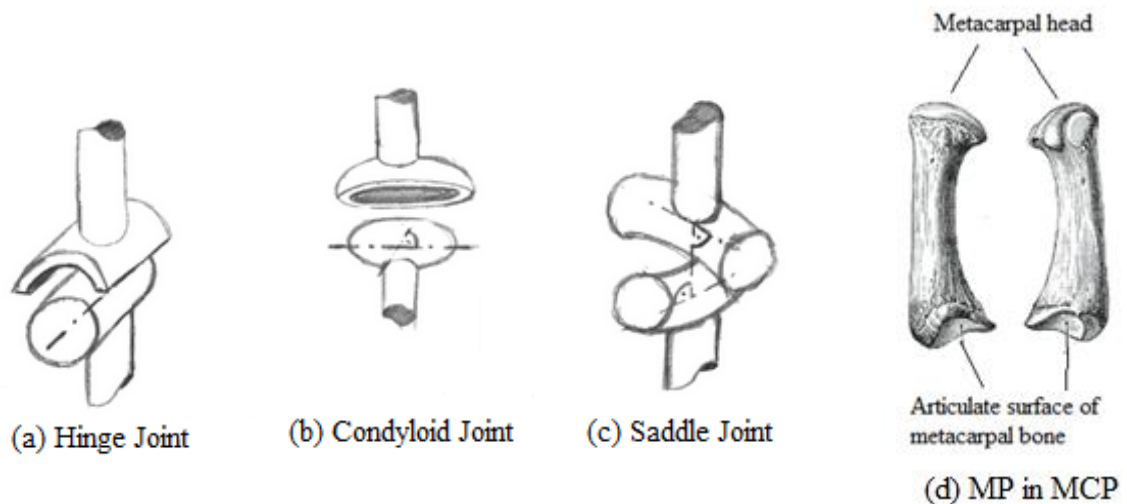


Figure 10. Joint types in a human hand. (a), hinge joint; (b), condyloid joint; (c), saddle joint; (d) is the articulate surface of the metacarpal bone in MCP joint exhibiting a condyloid joint (Grebenstein 2014, p. 43-44.)

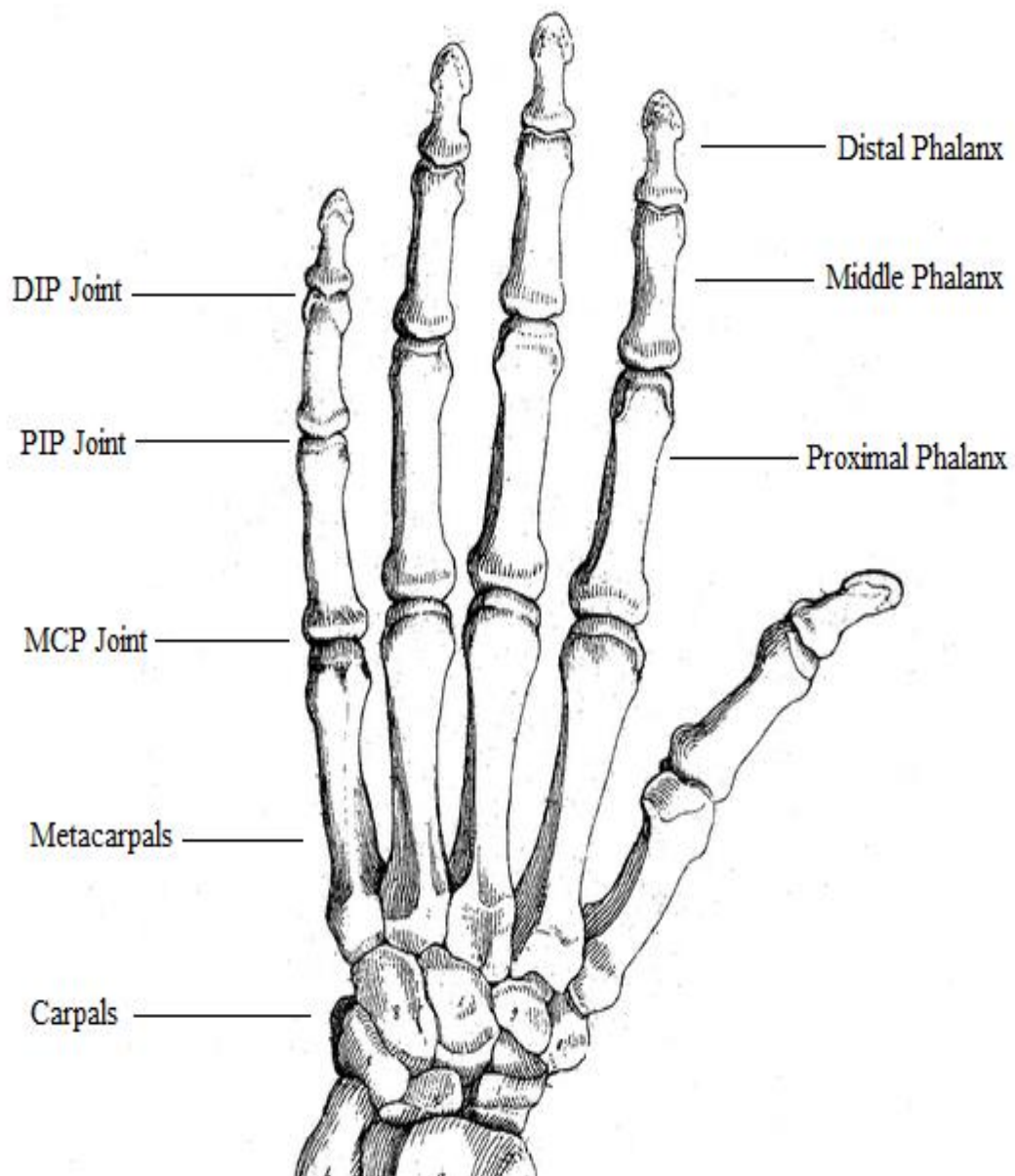


Figure 11. The bones and joints of the human hand (Schadow 2009.)

Because the human hand consists of five poly-articulated fingers, it is liable to deformation (Tubiana, Thomine & Mackin 1998, p. 4). These hugely depend on the shape of the joints in the finger. The different finger shapes also vary the DOF in each joint while the unique alignment of CMC joint in thumb offers greater range of motion (ROM) and flexibility (Hollister et al. 1995). In a natural resting position, without any active muscle contraction, the wrist is extended in 20° in neutral radial/ulnar deviation. The range of joints in the human hand skeleton in resting and flexion positions are shown in Table 1 below.

Table 1: The range of different joints in fingers excluding thumb (modified from: Barr & Bear-Lehman, 2001)

Position	Joints		
	MCP	PIP	DIP
Resting	45° approx.	30° - 45°	10° - 20°
Flexion	90° approx.	110°	90°

However, the range of flexion differs widely among persons and their hand structure. Also, the extension of MCP joints is observed go beyond 0°, vividly due to the ligament laxity. On the other hand, human hand consists of 29 muscles controlling the movement of the human hand. They are categorized into extrinsic muscles, that mostly control the extension and flexion of the digits and intrinsic muscles that allow the free movement of each digit. The extrinsic muscles are originated from the bones in the arm and are replaced by tendons as they approach the wrist while the intrinsic muscle is located completely within the hand. (Jones & Lederman 2006, p.16.) Among total 9 extrinsic muscles, 3 contribute to flexion or finger, 5 contribute to the extension of fingers and 1 contributes to the abduction of the thumb. Towards the base of PP, two groups of muscles called dorsal interossei (DI) and palmar interossei (PI) are originated that extend up to PIP and DIP joints. These DI and PI muscles abduct and adducts, and produce rotation at MCP joint. The movements of the PIP and DIP are functionally coupled due to the interaction between the extrinsic and intrinsic muscles.

Ligaments are fibrous tissues connecting a bone to another bone. They occur in joints and play a vital role in preventing abnormal movement in the joints (Figure 12(a)). However, due to their swollen structure, the modeling of HE becomes difficult as it increases uncertainty in the axis of rotation. On the other hand, tendons connect muscles to bone. The extensor tendons arise from the backside of forearm bones and allow each finger joint to straighten. Tendons are an important factor determining the stress force of the hand-finger grip.

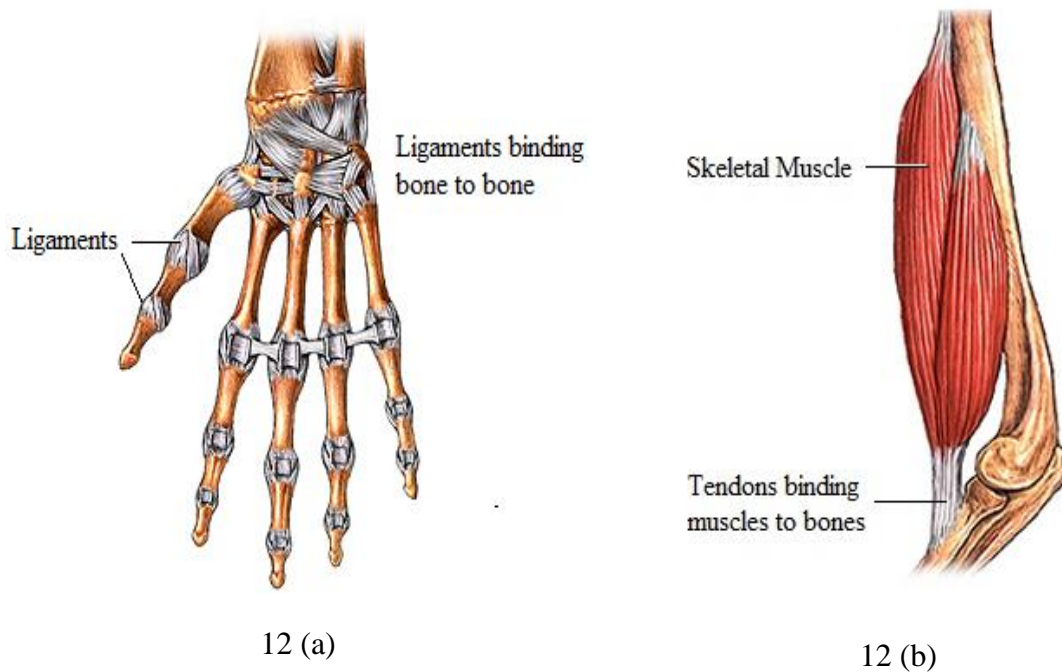


Figure 12.(a) The ligaments connecting bone to bone and (b) tendons connecting muscles to bone (Vorvick 2016).

2.3.2 Mathematical Modeling of Human Hand Finger

As the mechanism of HE vastly depend on the movement of the bones and joints in the fingers, many mathematical methods have been proposed to mimic the movement. Allen-Prince and Walton (Allen-Prince & Walton, 2011) modeled the motion of finger using law of force and acceleration. This model, however, was designed without consideration of complex human hand movements. The human hand movement is spatial, whereas, the finger follows planar. Thus the human hand-finger movement can be modeled mathematically using simple planar three-link manipulator (Rahman et al. 2014).

Consider a three-link planar manipulator as shown in Figure 13 represents the human finger (not thumb). The three joints (starting at the base) represents the MCP, PIP, and DIP and links L_1 , L_2 and L_3 represents PP, MP and DP. The D-H parameter table of the mechanism can be expressed as in Table 2 below. (Craig, 2005, p. 109.)

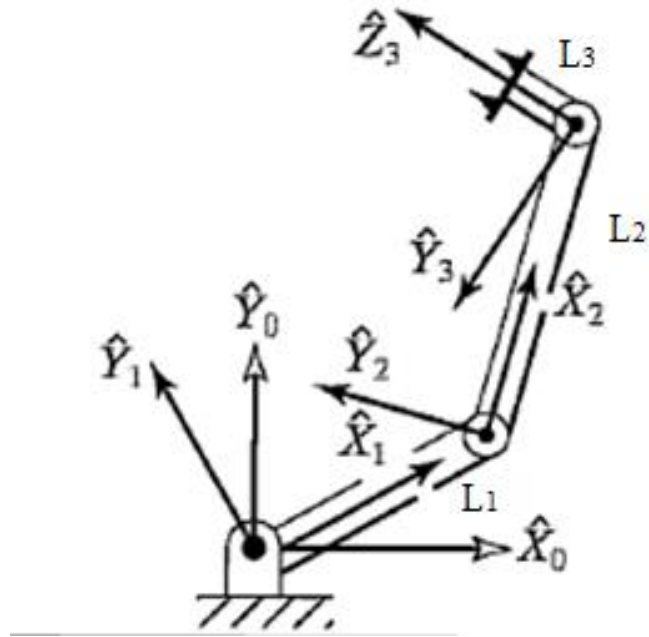


Figure 13. The three link planar manipulator mimicking the human index finger (Craig, 2005, p. 109)

Table 2: The D-H parameter table of the above mechanism (Craig, 2005, p.71).

Link	α_{i-1}	a_{i-1}	d_i	θ_i
1	0	0	0	θ_1
2	0	L_1	0	θ_2
3	0	L_2	0	θ_3

Where,

α_{i-1} : is the twist angle from Z_{i-1} to Z_i along X_i

a_{i-1} : is the distance from intersection of Z_{i-1} and X_i to the O_i along X_i

d_i : is the distance from intersection of Z_{i-1} and X_i to the joint along Z_{i-1}

θ_i : is rotation angle from of X_{i-1} and X_i to the joint along Z_{i-1}

Based on the table above, the forward kinematics can be solved as:

$${}^0_3T = \begin{bmatrix} C_{123} & -S_{123} & 0 & C_1L_1 + L_2C_{12} \\ S_{123} & C_{123} & 0 & S_1L_1 + L_2S_{12} \\ 0 & 0 & 1 & 0 \\ 0 & 0 & 0 & 1 \end{bmatrix} \quad (1)$$

Similarly, the inverse kinematics gives the fingertip position and orientation. The equation can be expressed as:

$${}^0_3T = \begin{bmatrix} C_\varphi & -S_\varphi & 0 & x \\ S_\varphi & C_\varphi & 0 & y \\ 0 & 0 & 1 & 0 \\ 0 & 0 & 0 & 1 \end{bmatrix} \quad (2)$$

Algebraically, we come out with the four nonlinear equations.

$$C_\varphi = C_{123} \quad (3)$$

$$S_\varphi = S_{123} \quad (4)$$

$$x = C_1L_1 + L_2C_{12} \quad (5)$$

$$y = S_1L_1 + L_2S_{12} \quad (6)$$

Based on these equations, the respective joint variables ($\theta_1, \theta_2, \theta_3$) can be solved.

$$\theta_1 = A \tan 2(y, x) - A \tan 2(k_2, k_1) \quad (7)$$

Where,

$$k_1 = l_1 + l_2C_2$$

$$k_1 = l_2S_2$$

$$\theta_2 = A \tan 2(S_2, C_2) \quad (8)$$

Where,

$$C_2 = \frac{x^2 + y^2 - L_1^2 - L_2^2}{2L_1L_2} \quad (9)$$

For a hand-finger model, the right-hand side value of equation 9 is always between -1 and 1. The physical interpretation of the values beyond these number is that the DP is abnormally away from the actual finger position which is not our case.

$$S_2 = \pm\sqrt{1 - C_2^2}$$

And,

$$\theta_3 = A \tan 2(S_\varphi, C_\varphi) == \varphi - (\theta_1 + \theta_2) \quad (10)$$

The equations 7, 8 and 10 gives the rotation angles in MCP, PIP and DIP joints in the human finger. However, the angles θ_1 , θ_2 & θ_3 are always in the range as described by table 1 above.

3 THE DESIGN

3.1 Materials

Two different materials are chosen for the HE structure and the actuator. To meet the requirement of strong and lightweight design, the HE structure uses PA 2200 polyamide. This material has high strength and stiffness and resistance to temperature and chemical. The properties can be found in Table 3 below.

Table 3: Properties of the PA 2200 used in the design of the HE (Shapeways 2017).

Properties	Value	Units
Density	0.45	g/cm ³
Tensile Modulus	1700	MPa
Tensile strength	48	MPa
Elongation at break	24	%
Flexural Modulus	1500	MPa
Flexural strength	58	MPa
Charpy-Impact strength	53	kJ/m ²
Shore D - Hardness	75	-
Melting point	172-180	°C

Similarly, the material for the actuator is a shore A30 silicone. The material is a hyper-elastic and elongates more than 450% of its original size. It is resistive to radiation, and dilute base or acid and has a functional temperature range of -55°C to 180°C. The typical properties of the material used can be seen from Table 4 below.

Table 4: Properties of the Silicone Shore A30 in the actuator (ACEO 2017).

Properties	Inspection Method	Value
Hardness	ISO 7619-1	30 SHA
Density	DIN EN ISO 1183-1A	1.10g/cm ³
Tensile strength	ISO 37 Type 1	>6 N/mm ²
Elongation at break	ISO 37 Type 1	>450 %
Tear strength	ASTM D 624 B	>15 N/mm
Tear strength	DIN ISO 34-1-A	>5 N/mm
Rebound resilience	ISO 4662	60%
Compression set	DIN ISO 815-1 Type B (22h/175°C)	<15%

Furthermore, the materials have following properties suitable for the design of actuator (Table 5).

Table 5: The typical characteristics of the Silicone Shore A30 in the actuator (ACEO 2017).

Characteristics	Inspection Method	Value
Limiting Oxygen Index	EN ISO 4589-2/ ASTM D2863	25%
Dielectric strength	IEC 60243-1	25kV/mm
Volume resistivity	IEC 62631-3-1	$6.4 \times 10^{15} \Omega \text{ cm}$
Dielectric constant (50 Hz)	IEC 60250	2.8 ϵ_r
Dissipation factor (50 Hz)	IEC 60250	$2 \times 10^{-4} \tan \delta$

3.2 Hand ExoskeletonFrame Structure

The designed HE includes 6 individual solid parts constrained by 5 joints as shown in Figure 14 below. When worn, the parts P1, P2, and P3 fit the DP, MP and PP in human finger respectively. Similarly, the part P4 associates the parts P5 and P6 that fits into the palm and holds the HE. The first three joints, J1, J2, and J3 are revolute and individually follows the DIP joint, PIP joint and MCP joints. These joints are designed to follow the natural finger range and forbid any unusual or potential hazardous motion. The J4 is a revolute joint that maintains comfortable wearing experience in the palm. Finally, the J5 is a translation joint performing two distinct tasks. First, it helps to match the length of HE digits with human fingers during extension and flexion, second, allows the flexibility to fingers in sideways movement. The CAD modelling is made with Solidworks.

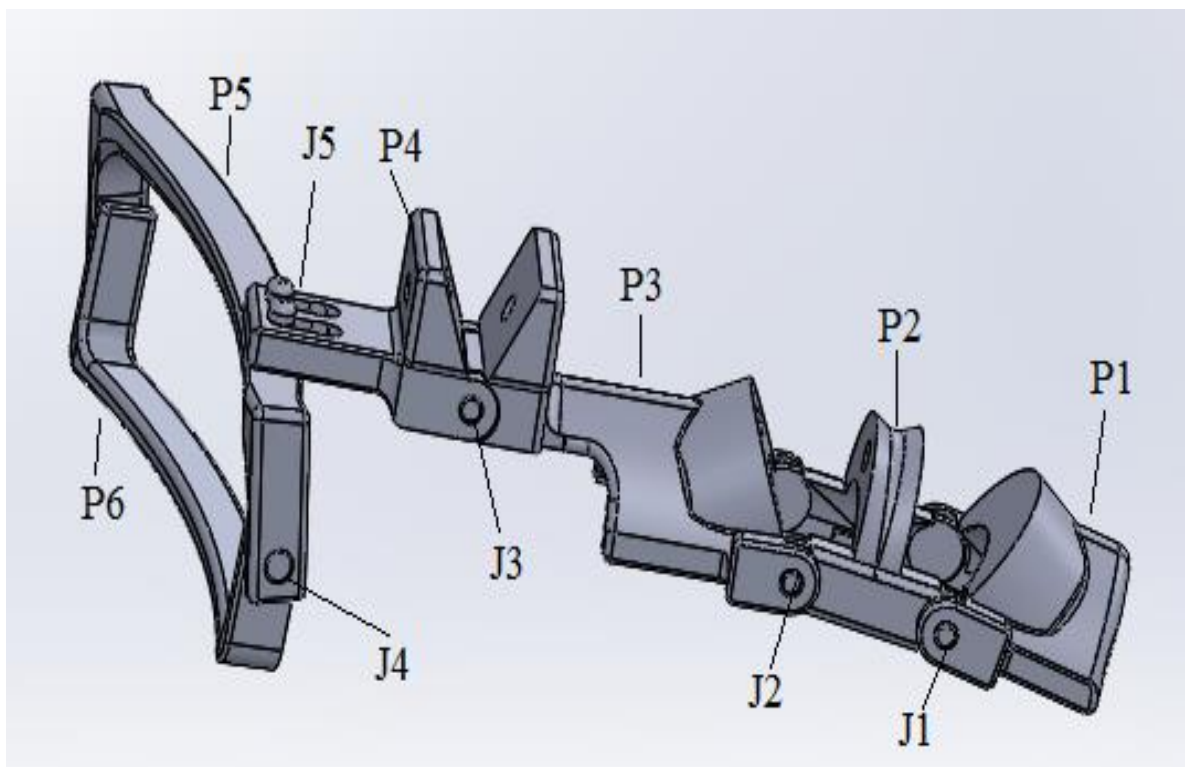


Figure 14.The CAD model of the designed HE model

The HE model is 3D printed with lightweight “strong and flexible” plastic as described earlier in this chapter. As a result, the printed 3D model is lightweight and fits well in the hand. The model smoothly follows the corresponding joints and digits as shown in Figure 15 below. The revolute joints J1, J2, J3, and J4 is helped to adjust the rotation of finger

digits. While the translation joint J5 plays a key role in adjusting the length during extension and flexion of the finger.

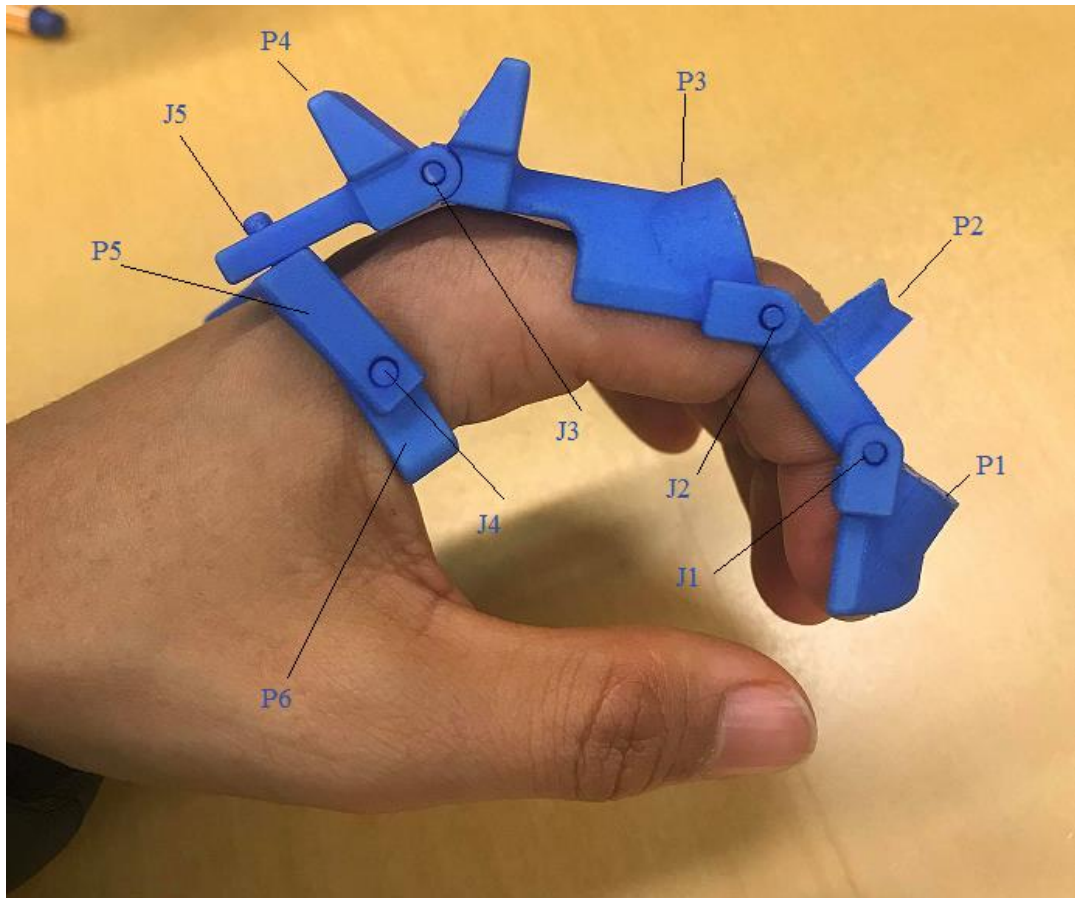


Figure 15.The 3D printed model of the designed HE model.

Similarly, the 3D printed model of HE achieves the rotational displacements as per required by the human biomechanics. The degree of movements achieved by the 3D printed model as when worn are presented in Table 5 below.

Table 5: The movements allowed by the joints

	Joints				
Maximum	J1	J2	J3	J4	J5
Rotation	75°	60°	45°	270° (un-worn)	10° (each left/right)
Translation	0 mm	0 mm	0 mm	0 mm	5 mm (front-back)

3.3 Actuator Structure

To match the HE, two individual soft rotary actuators with silicone (hardness SHA 30) at the DIP and PIP joints are designed. These actuators extend or flex the phalanges to achieve opening and closing movement of fingers. The actuators are designed to follow the rotary motion to match the revolute nature of the finger joints. One edge of the actuator is inclined to approximately 62° along the X-axis while its opposite edge is kept 90° along the same axis. Similarly, the upper dimension of the actuator is designed bigger than the lower to achieve the rotary motion during the function. On the other hand, the DIP joint actuator has only one opening for air inlet or outlet (Figure 16) while, the PIP joint actuator consists 2 openings for air flow (Figure 18). The DIP joint actuator is the last air chamber thus requires single opening whereas, the PIP joint actuator acts as a bridge between the source and DIP joint actuator thus requiring two openings. Despite this difference, the overall dimensions of these two actuators are same (Figure 17).

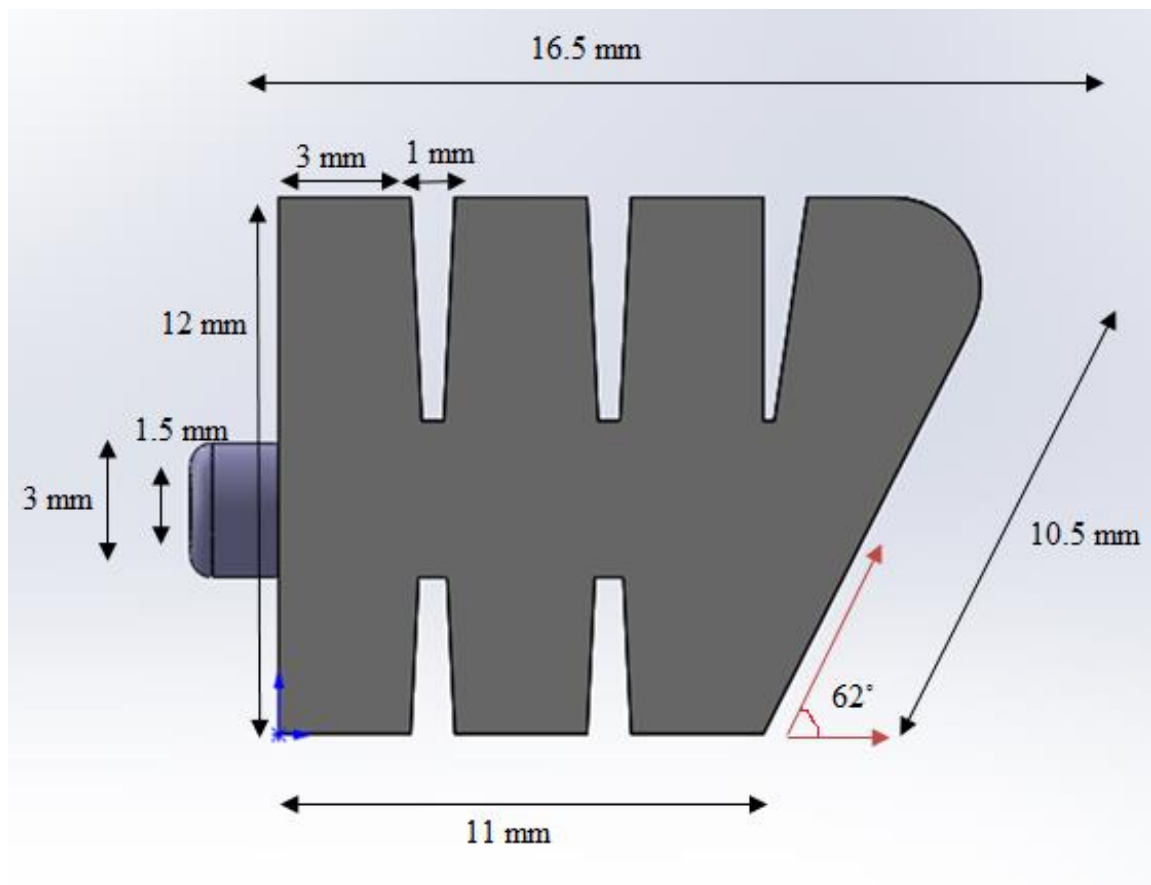


Figure 16. The side view of DIP joint rotary actuator in the HE.

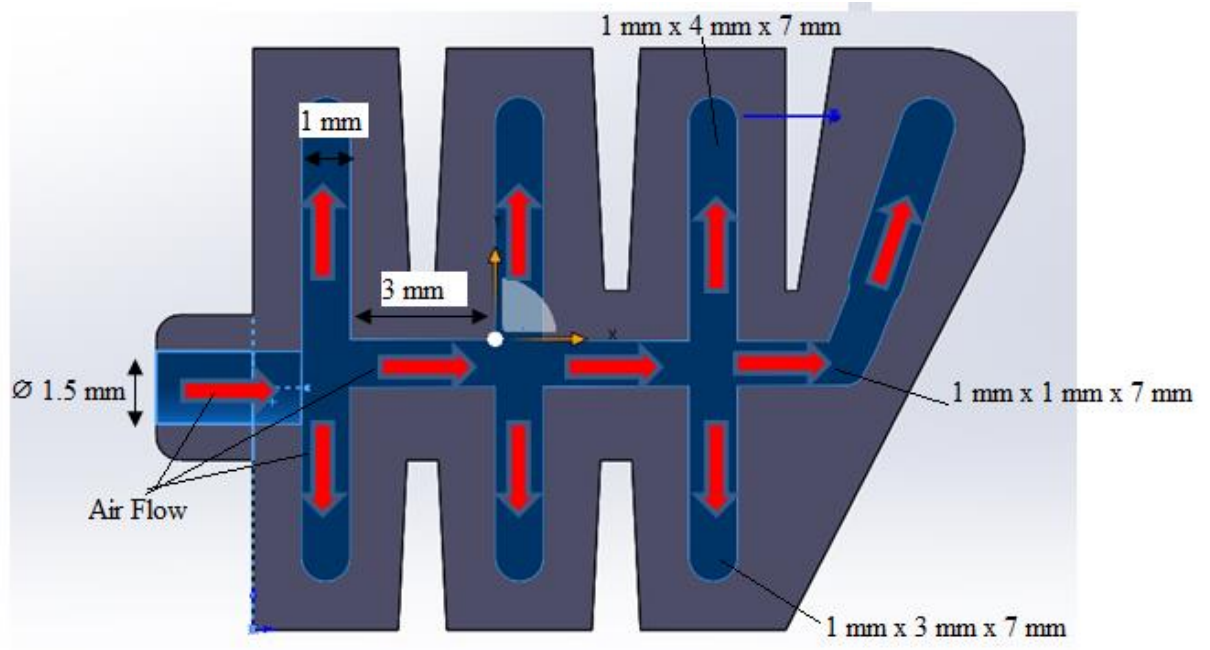


Figure 17. The cross-section view of DIP joint rotary actuator in the HE. The internal and external dimensions of DIP and PIP actuators are same.

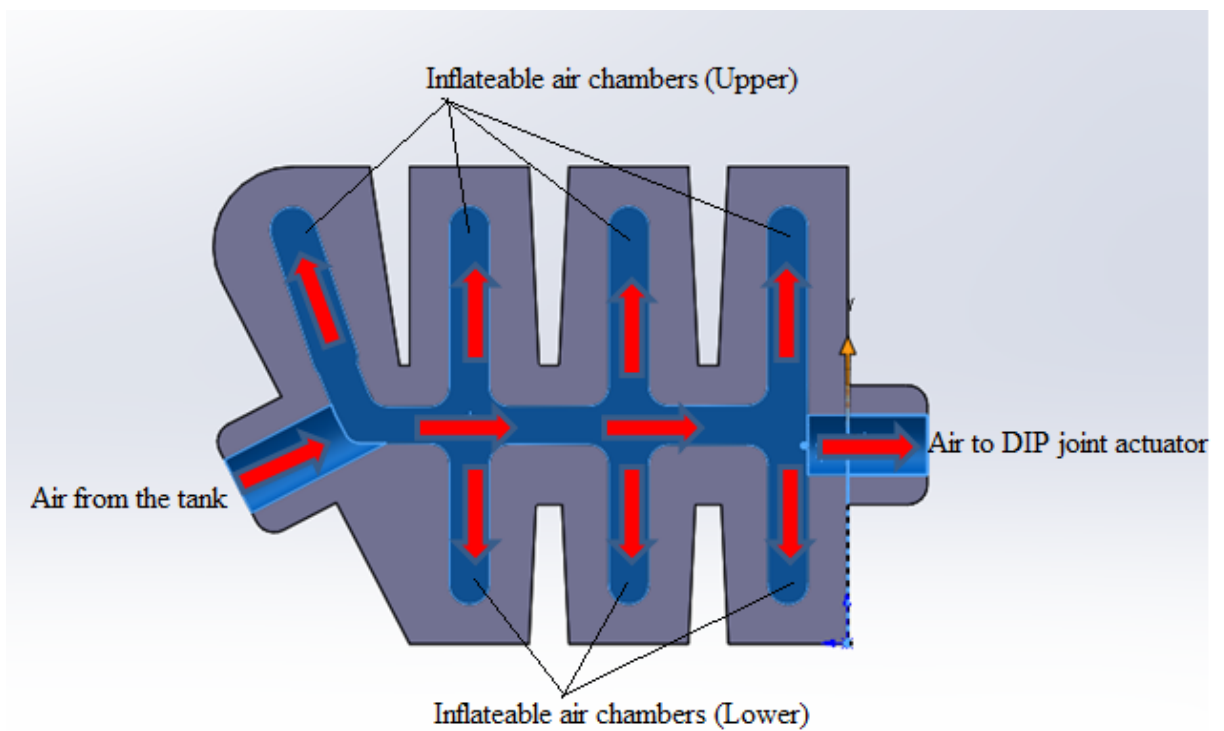


Figure 18. The cross-section view of PIP joint rotary actuator in the HE

The actuator dimension is chosen as to meet the functionality of the HE. Based on the principle that extension at the top is greater than the extension at the bottom, four air chambers are designed at the top to achieve bigger displacement than the lower with 3 air chambers. The overall characteristics/dimensions of the actuators are presented in Table 6 below.

Table 6: The overall characteristics/dimensions of the silicone (SHA 30) actuators

Characteristics/dimensions	Actuators	
	PIP	DIP
Upper length	16.5 mm	16.5 mm
Lower length	11 mm	11 mm
Contact Edges	12 mm × 20 mm at 90°/ 10.5 mm × 20mm at 62°	12 mm × 20 mm at 90°/ 10.5 mm × 20mm at 62°
No of inlet/outlet	2	1
Dimension of inlet/outlet	∅1.5 mm × 2 mm (inner)/ ∅3.0 mm × 2 mm (outer)	∅1.5 mm × 2 mm (inner)/ ∅3.0 mm × 2 mm (outer)
No of air chambers	4 upper/ 3 lower	4 upper/ 3 lower
Air chamber dimensions	1 mm × 4 mm × 7 mm (upper)/ 1 mm × 3 mm × 7 mm (lower)	1 mm × 4 mm × 7 mm (upper)/ 1 mm × 3 mm × 7 mm (lower)
Air passage dimensions	1 mm × 1 mm × 7 mm	1 mm × 1 mm × 7 mm
Edge to air chamber separation	1 mm	1 mm
Chamber to chamber separation	0.5 mm – 1 mm (max)	0.5 mm – 1 mm (max)

Based on the characteristics and dimensions mentioned, the final design of the HE was achieved as in Figure 19 below.

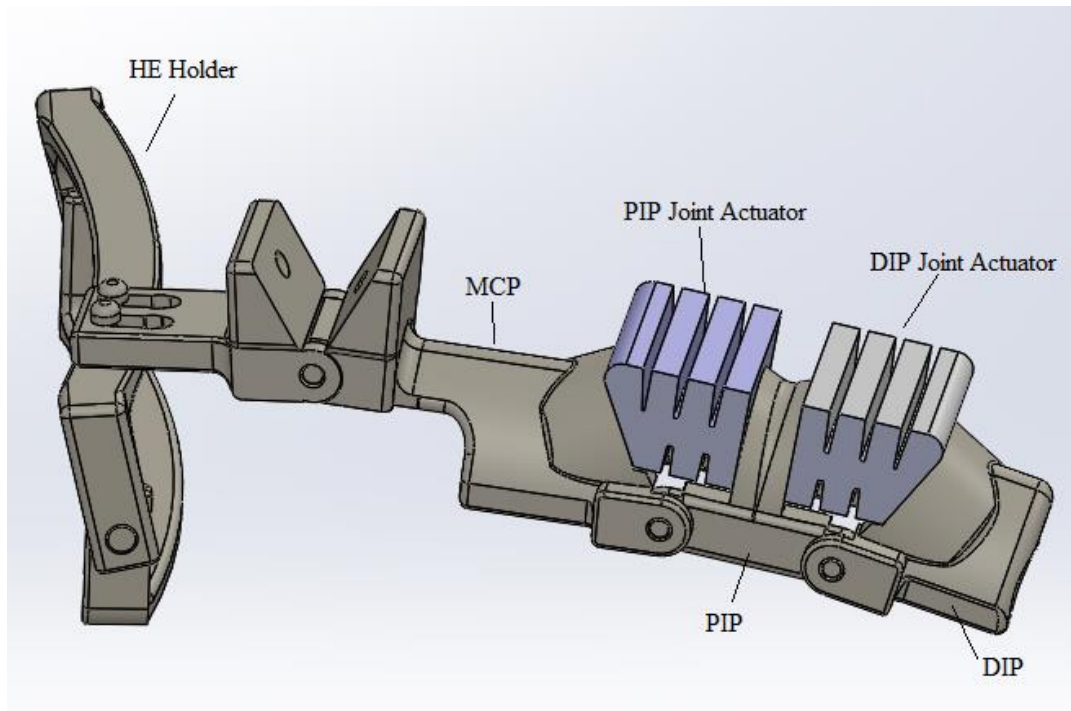


Figure 19. The final design of the HE in the project

Next, the air flow in the HE can be seen from the cross-section of the HE provided in Figure 20 below.

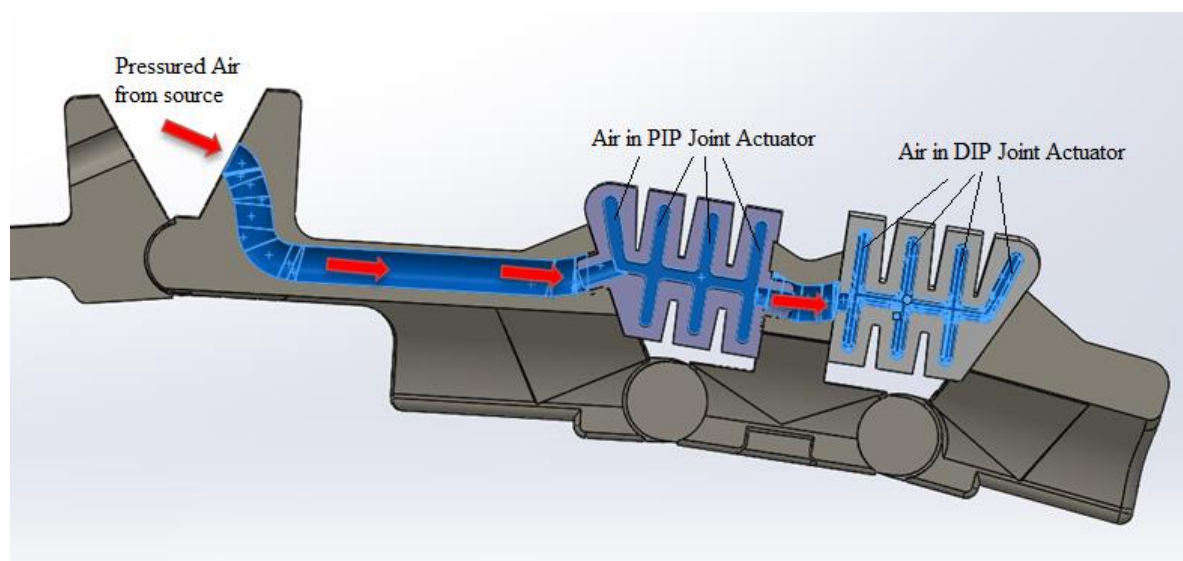


Figure 20. The cross-section dimensions of actuators.

3.4 The Control system

The HE is designed to follow extension and flexion of the digits with the air pressure supplied from the source. For this, a pneumatic line is created with an electric DC pump taken as a source. The unidirectional pump exerts the air pressure towards the HE via pressure gauge. The required pressure is maintained as per pressurization of both actuators. The extension in the HE is achieved with the inflation of actuators with the air pressure. The constant pressure is maintained for the required period. And once when the flexion is required, the pressure relief valve is opened thus releasing the pressure from the actuators. When the air pressure is fully released from the actuators, the actuators return to their normal position allowing flexion of the HE. The operation of the pump is controlled electrically via EEG signals in the BCAFO project. The Figure 21 below shows the schematic of the air pressure flow in the HE system.

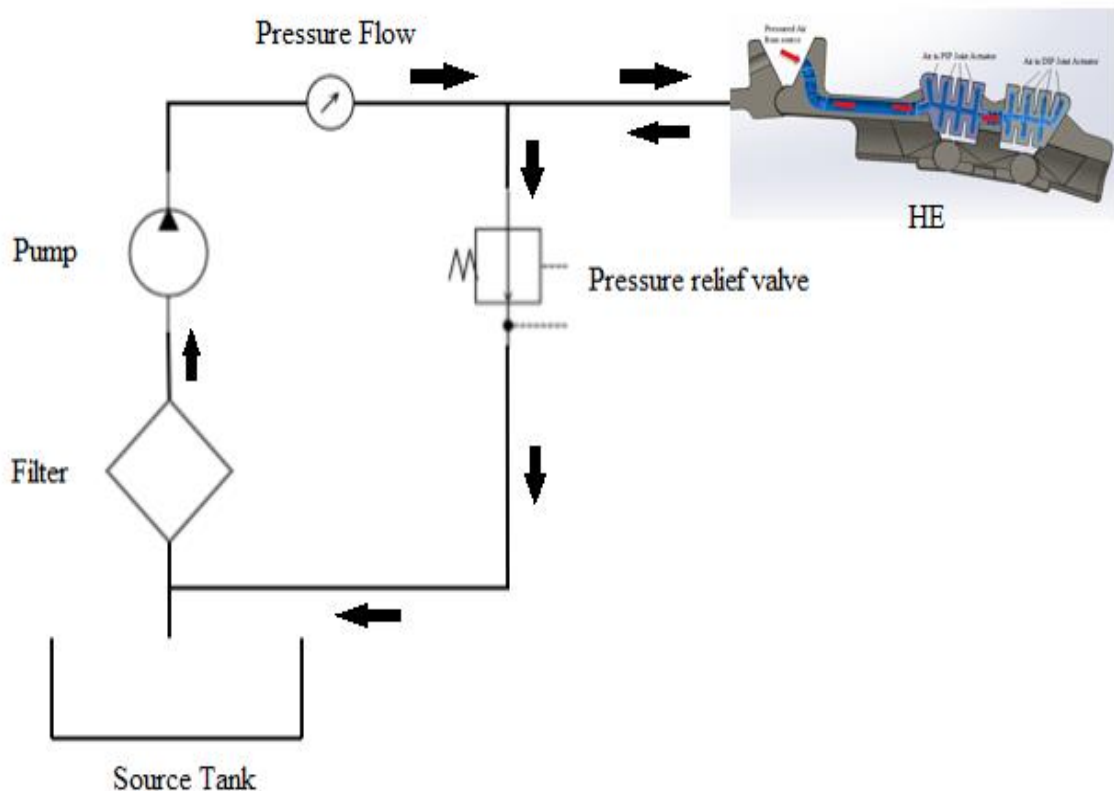


Figure 21. The schematic of the pressure flow in the HE system

The motor used in the research is a unidirectional 12 V DC motor. The pump is based on a theory of vacuum pump capable achieving a maximum vacuum of 420 mmHg which is enough for the research. The pump weight is approximately 50g which helps to make lightweight and portable system. The motor used in the project can be seen in the figure below (Figure 22).

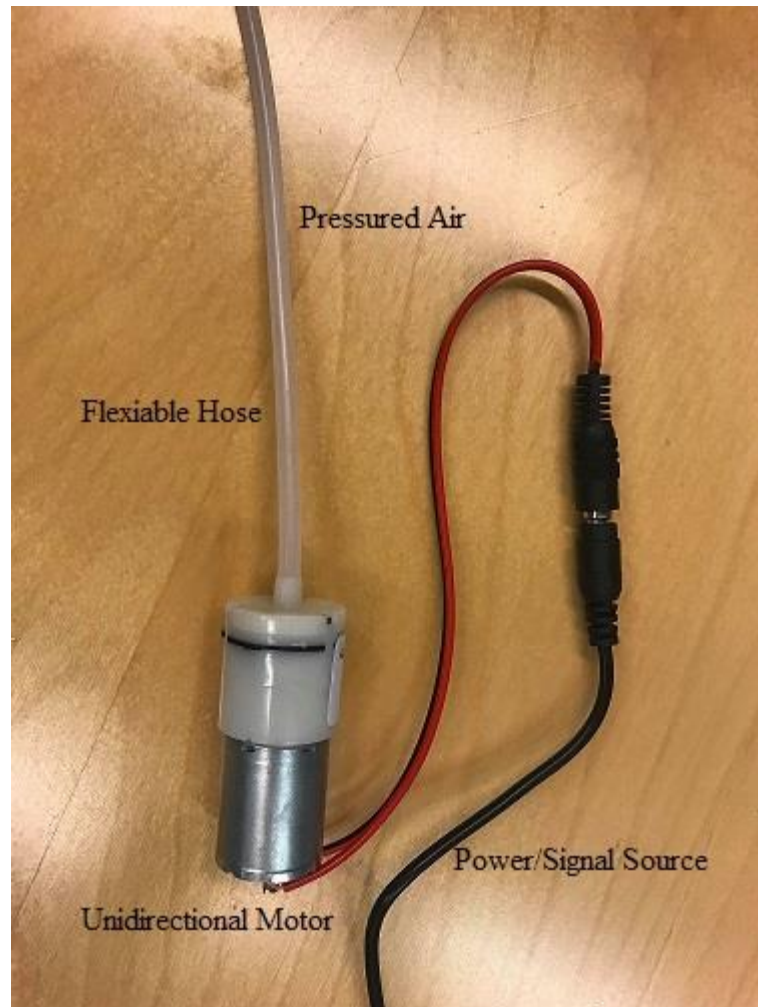


Figure 22. The unidirectional motor used in the research

4 RESULTS AND ANALYSIS

The result of the HE is mainly characterized by the performance of the HE frame and the silicone actuators at PIP and DIP joints. The HE frame provides the guided path for the natural movement of the hand. On the other hand, it constrains the unnatural movement that are potentially hazardous to the hand-finger biomechanics. Similarly, the silicone pneumatic actuators provide essential power to actuate the HE frame to achieve a finger-hand motion for its purpose of rehabilitation and ADL. The performance of these elements is discussed below.

4.1 Performance of HE frame structure

The analysis of the HE frame is made with the Adams 2014 software. The trajectory of the simulation result follows the desired path of the natural movement of the hand. The natural resting state of finger-position makes some small angle along the x-axis. This angle is divided in between DIP, MCP and PIP joints. The joints in HE frame forbid the digits to move in upward direction assuring the safety of the user. However, the downward motion is encouraged to achieve the flexion motion of the hand-finger. Figure 23 shows the natural resting position of an unactuated HE frame and Figure 24 shows the maximum extension position of the HE frame achieved with HE simulation in Adams 2014. The simulation was made for 15 seconds, in which 0 s represents the natural resting position.

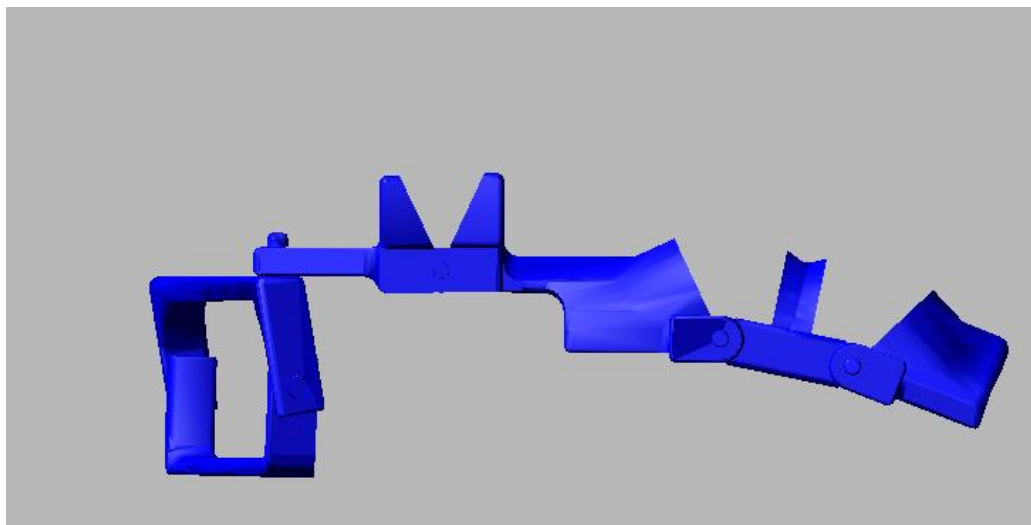


Figure 23. The natural resting position of unactuated HE frame achieved from Adams.

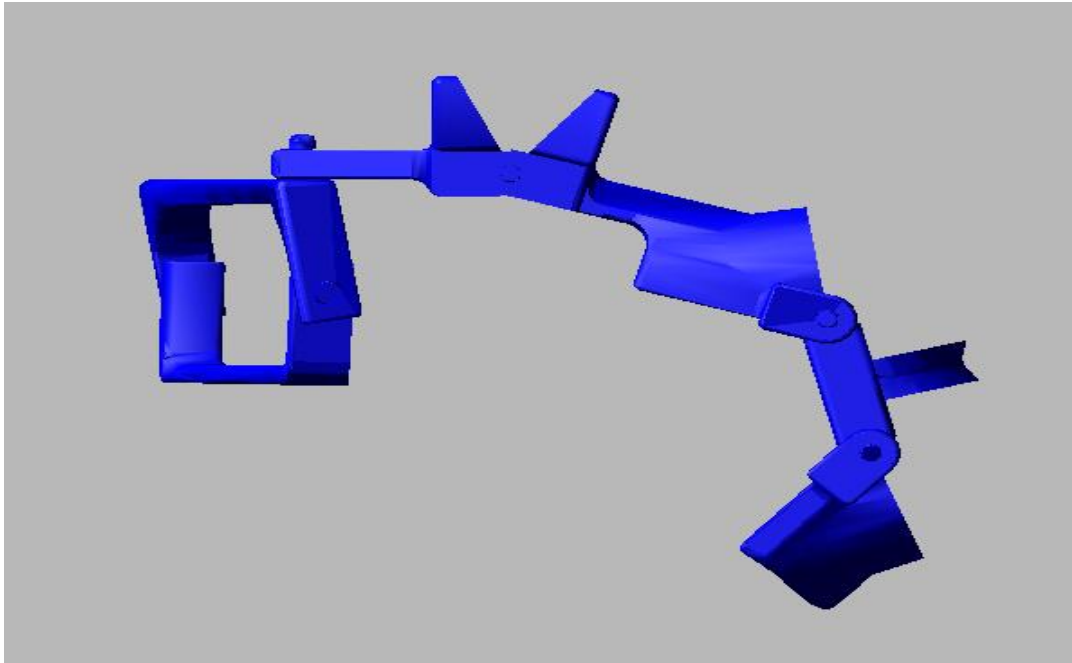


Figure 24. The maximum extension position of fully actuated HE frame achieved from Adams.

The rotations at different joints can be seen from Figure 25 below.

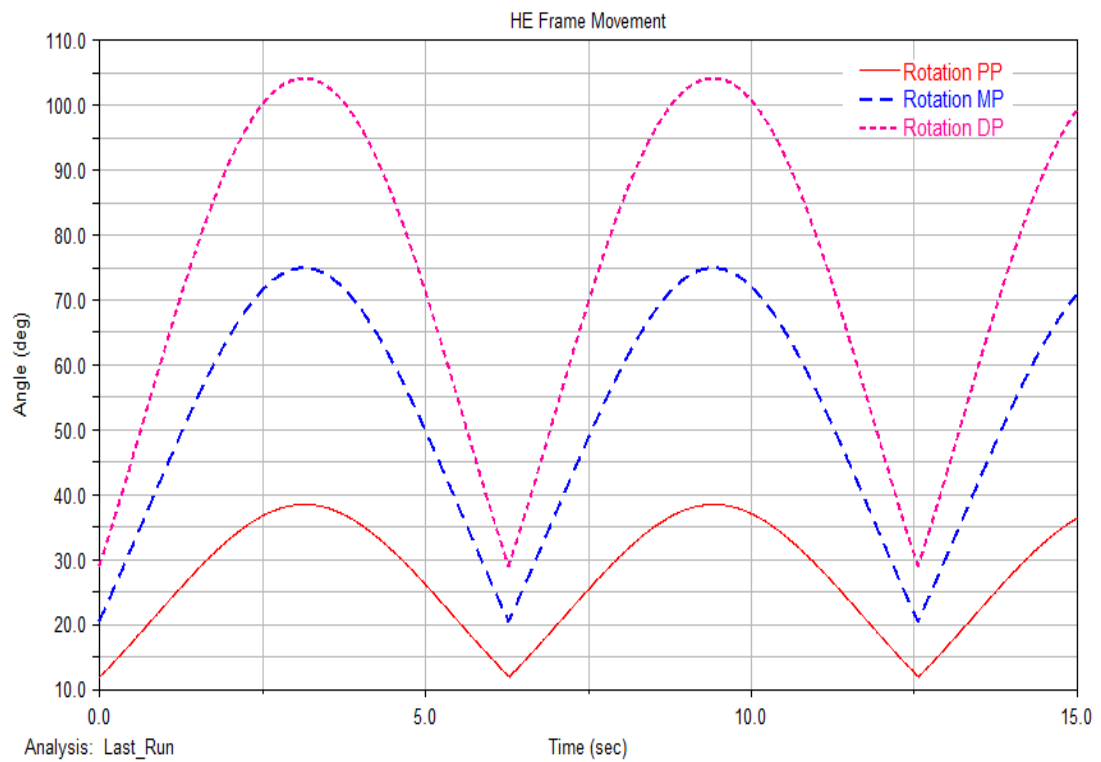


Figure 25. The rotation achieved by different joints in the HE frame

The graph shows that the rotation achieved by PP, MP, and DP at MCP joint, PIP joint and DIP joint are in ascending order. At resting position, the angle made by PP is 5° , MP is 20° and DP is 30° . However, when the extension is applied, the angles in each joints increases. The maximum rotation achieved by PP is 38° , MP is 75° and DP is 104° . This means, during the operation of the HE, the freedom of rotation achieved by PP is 33° , MP is 55° and DP is 74° .

On the other hand, Figure 26 shows the displacement achieved by each phalange in the finger.

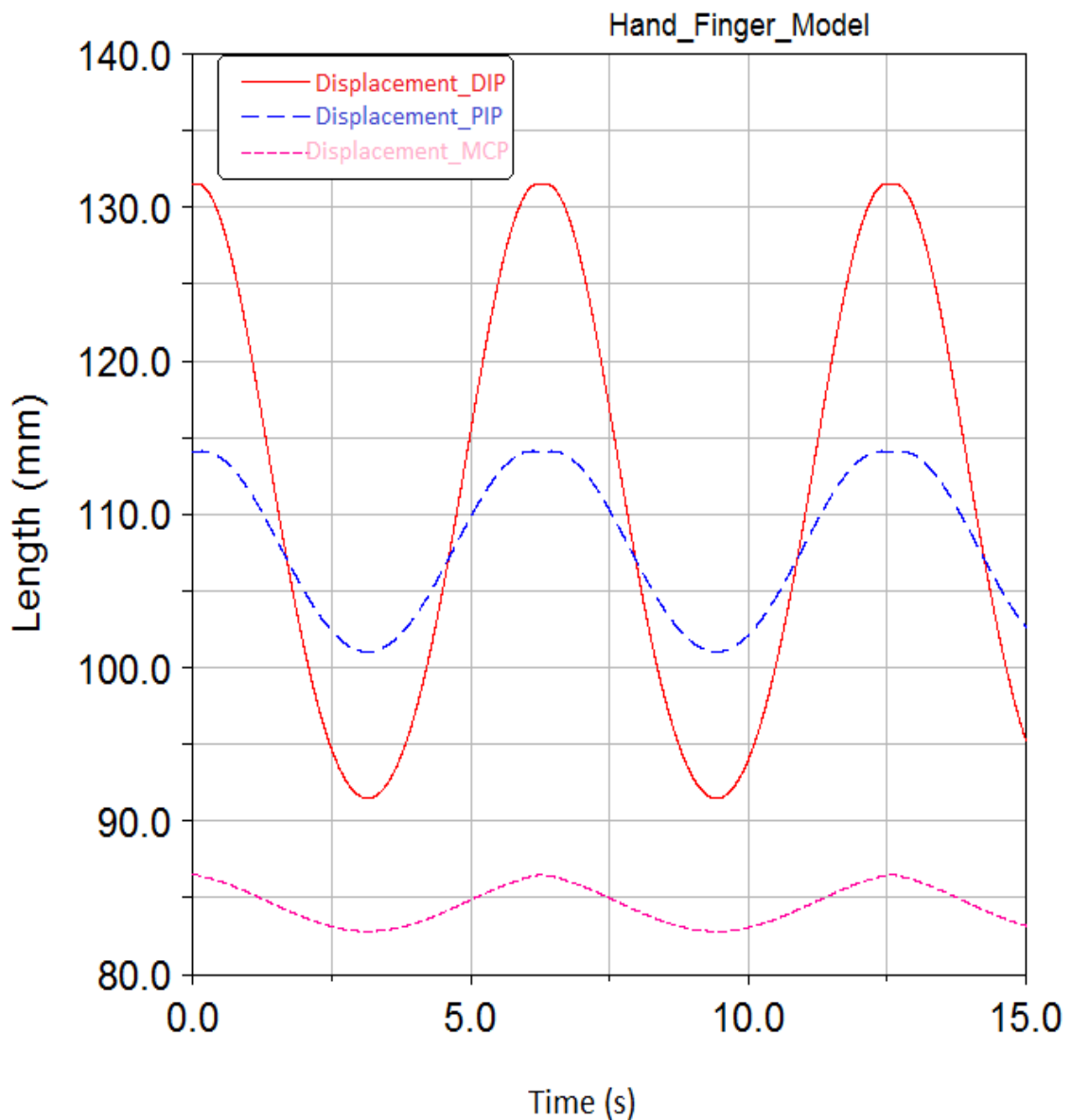


Figure 26. The displacement achieved by the different phalanges

The graph shows that the highest displacement is achieved by the DP followed by MP and PP. It can be seen that the average displacement for PP is 10 mm, MP is 30 mm and DP is 10 mm.

Similarly, Figure 27 shows the angular velocities achieved by phalanges during the simulation of HE frame for extension and flexion. During the extension, the graph converges together at a point meeting all at 0 rad/sec. Then the graph diverge away reaching different maximum angular velocities for different phalanges. During the process, the maximum angular velocity achieved by PP is 14 rad/sec, MP is 42.5 rad/sec and DP is 71.25 rad/sec.

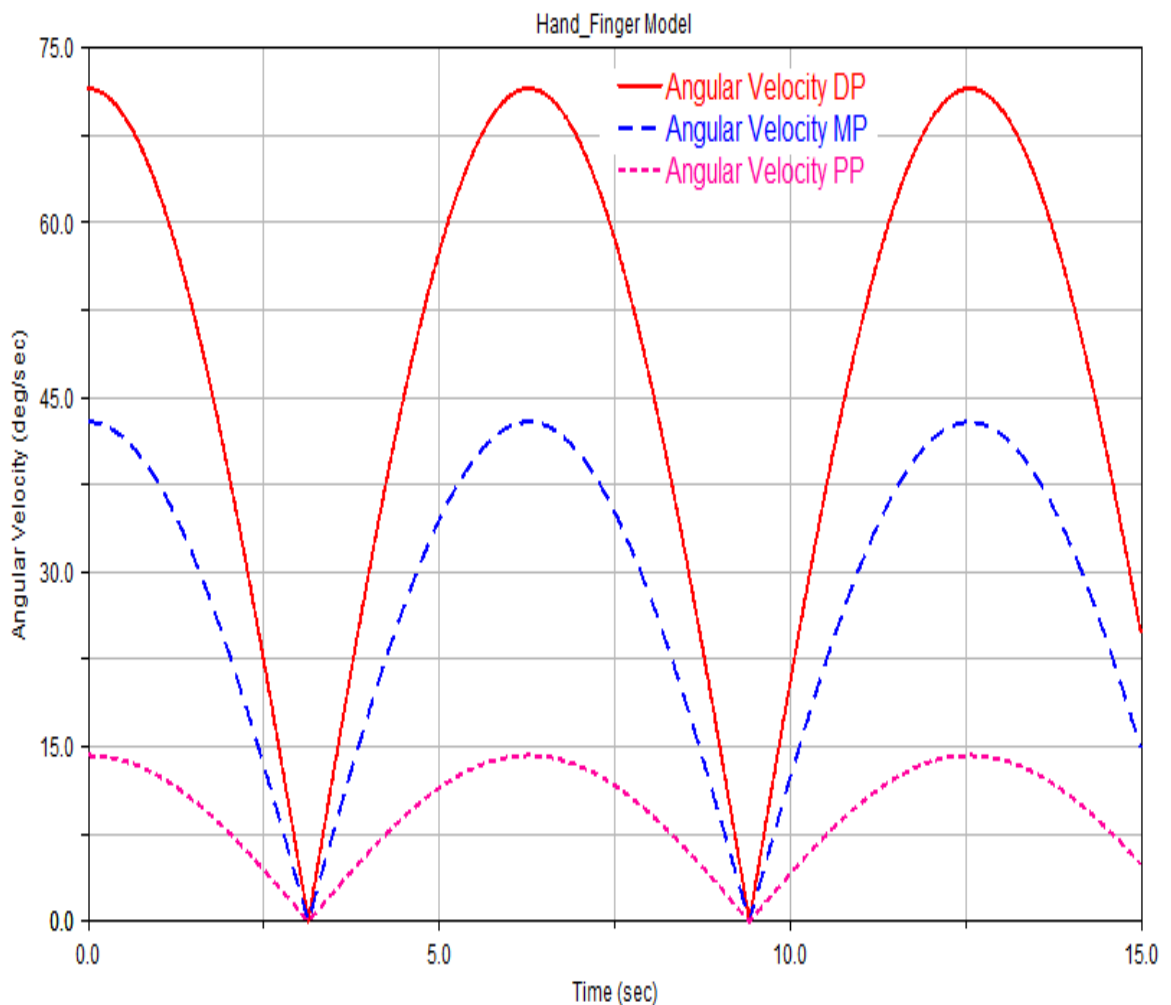


Figure 27.The angular velocity of DP, MP, and PP.

Similarly, in order to ensure the reliability of the HE frame, the static stress analysis is made with finite element method (FEA) using Ansys 2018. The analysis is made by creating a mesh of the 3D CAD assembly together with the actuators. Figure 28 shows the segment view of the FEA mesh model of the assembly.

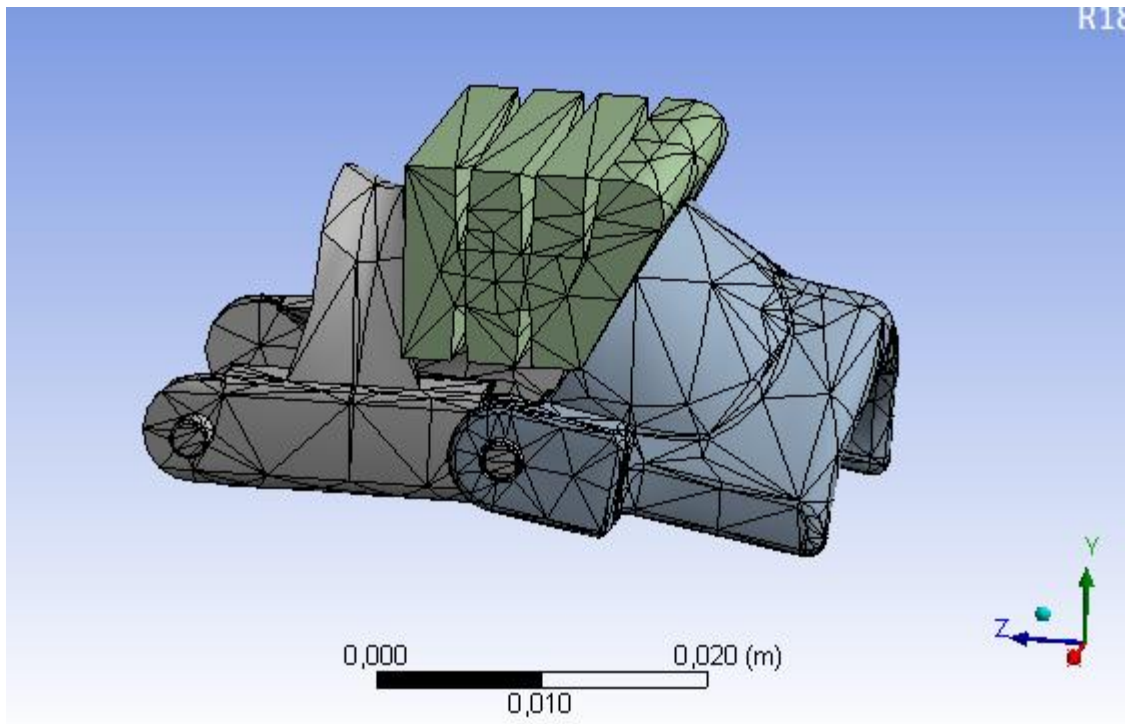


Figure 28. The FEA mesh model of the HE frame-actuator assembly of MP-DIP joint actuator-DP.

The result of the stress analysis of the simulation showed that the critical point is likely to occur in the joints due to the cyclic load and constant interaction. However, due to the strong material property of the PA 2200 polymer, the fatigue failure is unlikely to occur in the HE under operational pressure.

4.2 Performance of Actuators

Actuators are the fundamental source of torque transmission in the HE performing hand-finger extension and flexion. To do so, the pressurized air is pumped into the actuator by an air pump and released by a pressure relief valve constantly as described in the previous chapter. During the process, the soft silicone actuator inflates in a rotary motion because of

its design making the revolute motion between the joints. The hyper-elastic nature of the silicone helps to achieve the required continuous strain under the stress. Figure 29 shows the stress-strain graph of the actuator under biaxial, uniaxial and shear stress.

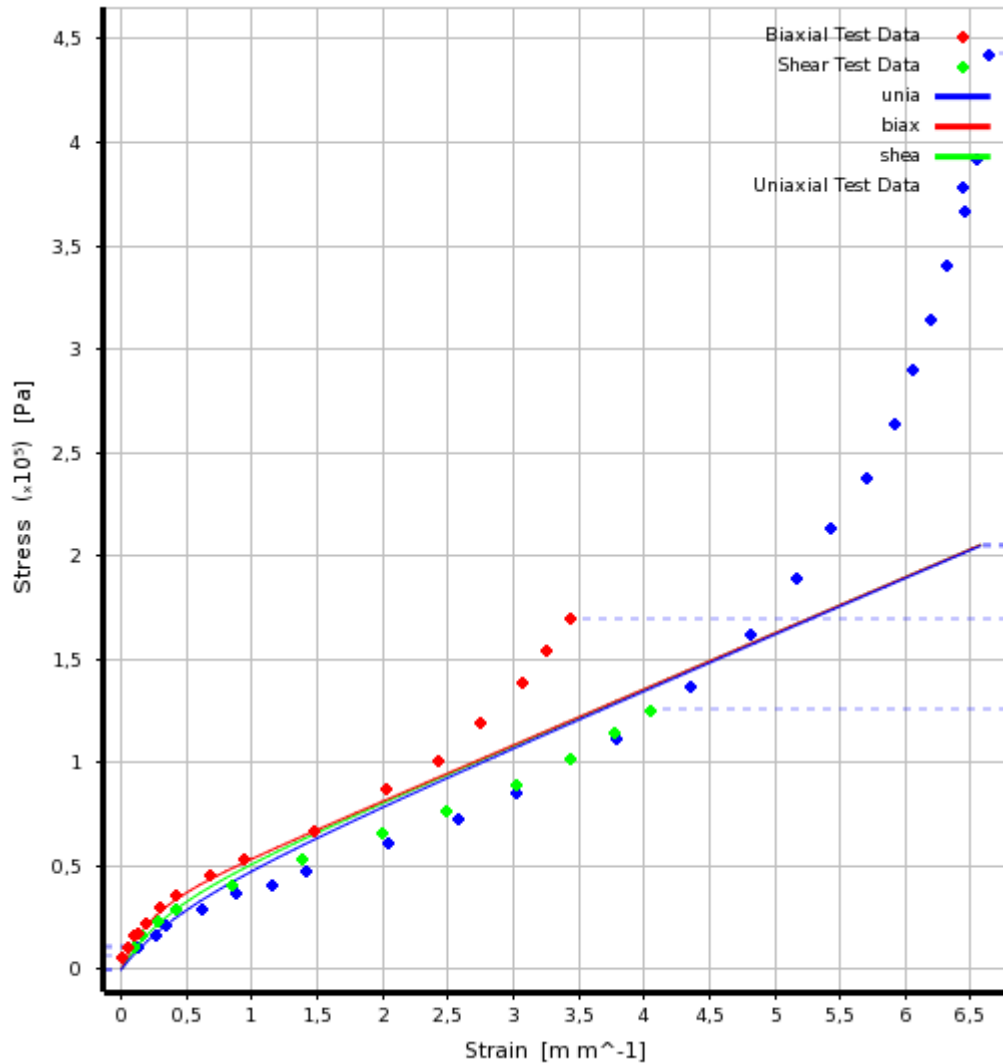


Figure 29. The stress-strain graph of the silicone SHA 30 actuator under biaxial, uniaxial and shear stress.

Based on the material properties, the simulation result is presented. When the pressure is fully applied to the actuator, the actuator undergoes deformation. During deformation, the strain in the actuator is achieved in the surface of the actuator. The deformation results in the displacement which is later transferred to the HE. Figure 30 and Figure 31 show the zero deformation and 100% deformation in the DIP joint actuator.

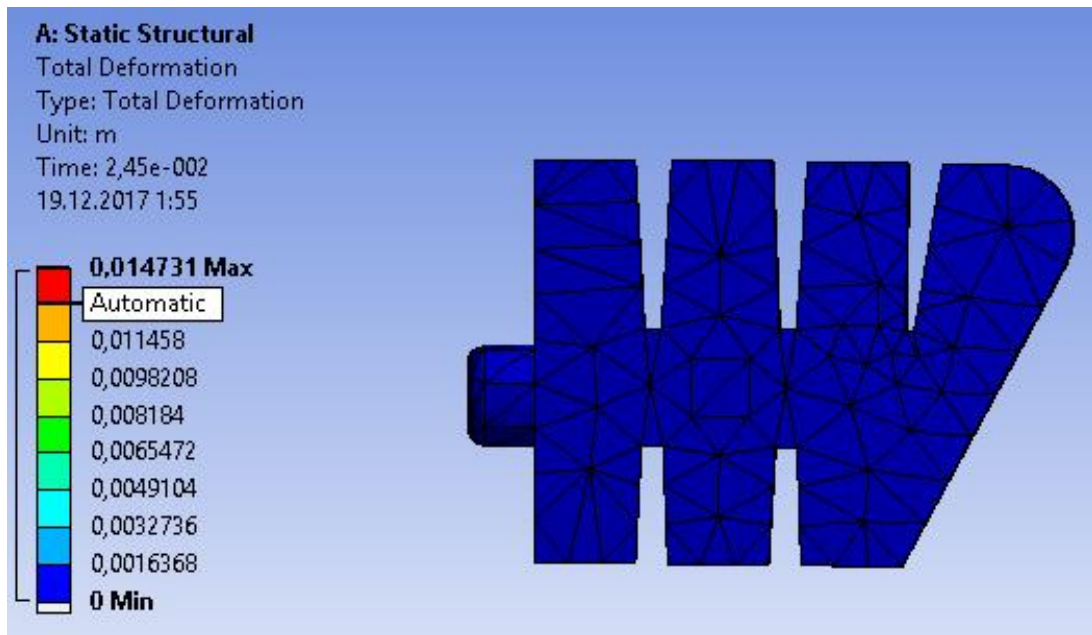


Figure 30. The zero deformation of the DIP joint actuator

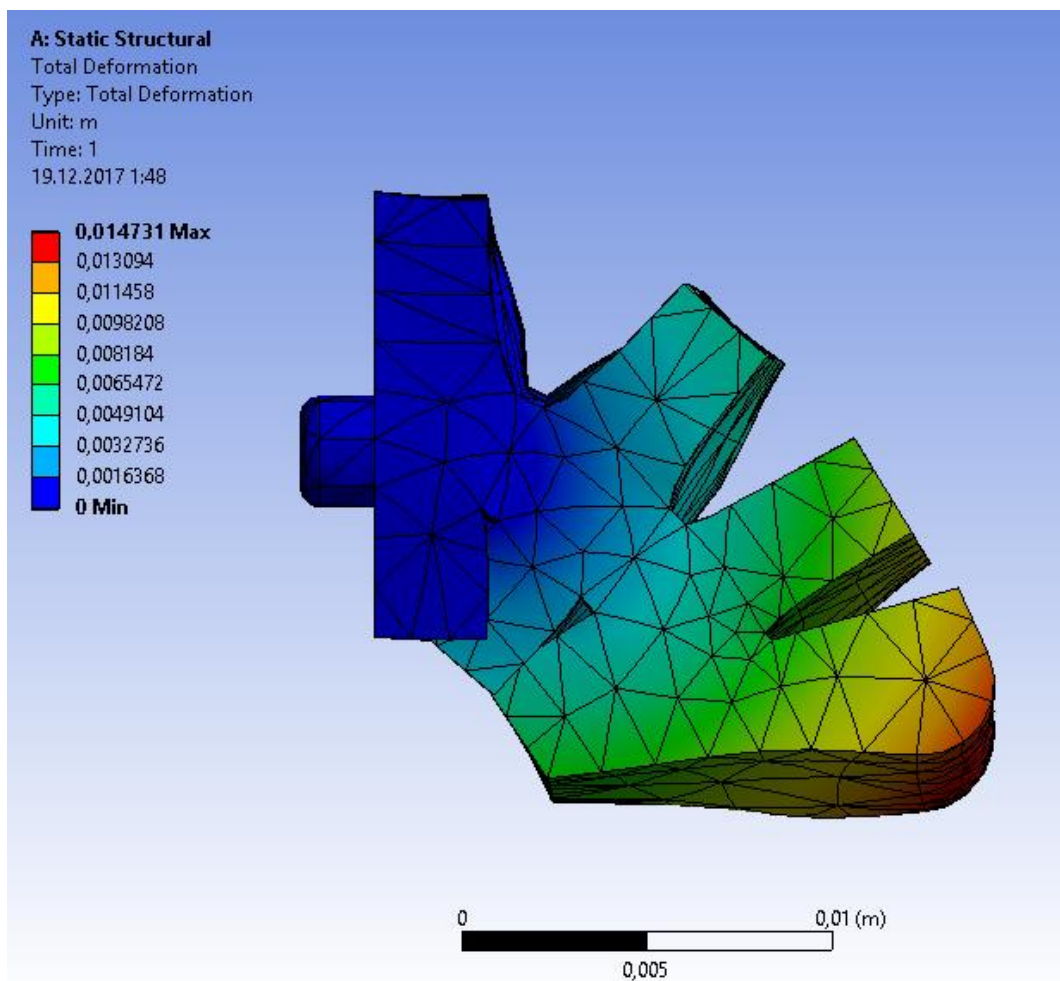


Figure 31. The deformation achieved by the DIP joint actuator.

The deformation in DIP joint actuator in Figure 31 can be illustrated graphically in Figure 32 below. The pressure is given for 1 s to reach full deformation as shown in the graph below. The result achieved is a linear deformation. It is found that the minimum deformation is 2.6506×10^{-4} m at 0.0245s and it increases linearly until it reaches maximum deformation of 1.4731×10^{-2} m at 1s.

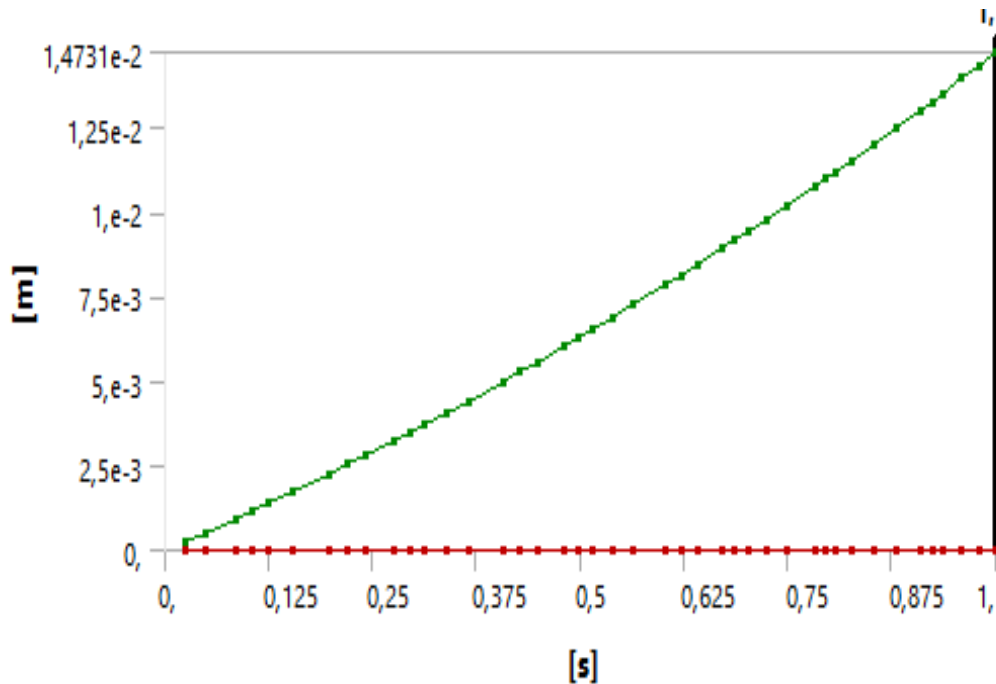


Figure 32. The graphical illustration of the deformation achieved by the DIP joint actuator

Similarly, the result of equivalent elastic strain is presented in Figure 33 below. The figure shows that the elastic strain increases linearly with increase in air pressure supply. From the graph, it can be seen that the maximum equivalent strain occurs at the full supply pressure. At this point, the maximum equivalent stress value is 0.46644 m/m. Due to this, the critical strain point occurs in the edge of the first air chamber as shown in the figure below. Similarly, the minimum equivalent stress occurs towards the opposite edge of the air inlet. The minimum value of the equivalent strain is 1.1159×10^{-6} m/m and occurs in the beginning when there is no air pressure supply. Likewise, Figure 34 shows the graphical illustration of the equivalent elastic strain achieved by the DIP joint actuator

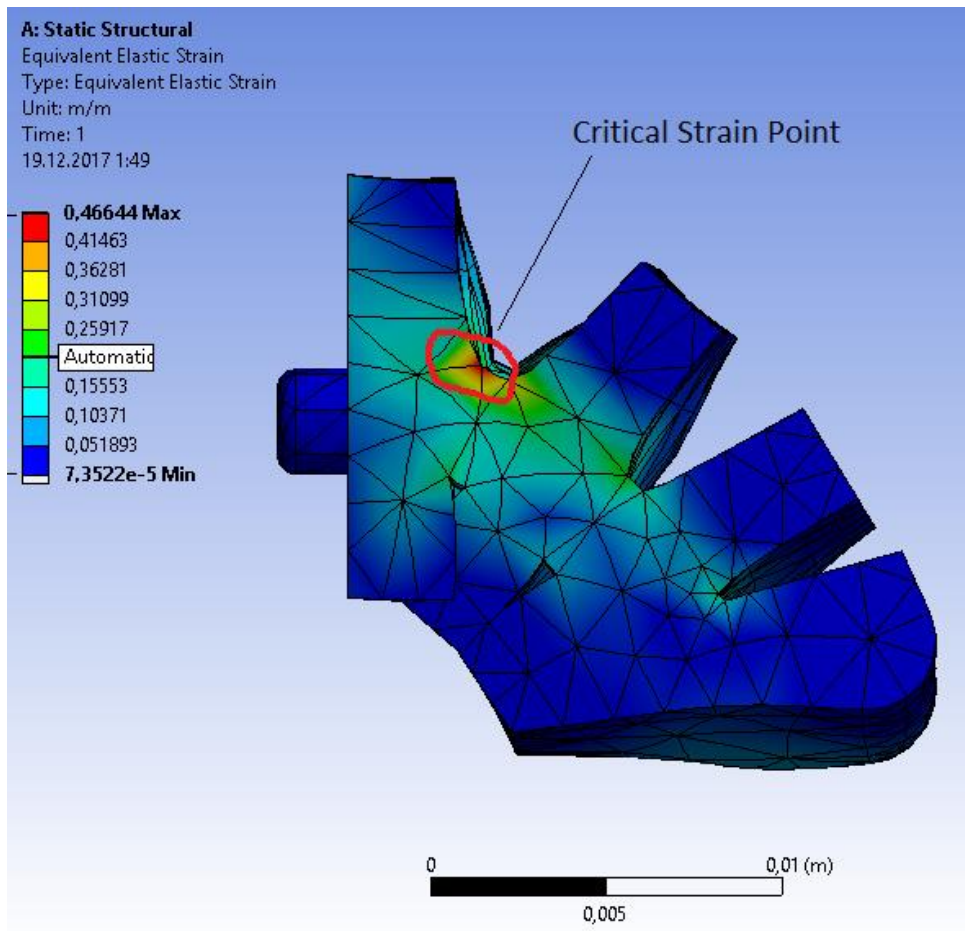


Figure 33. The equivalent elastic strain of the DIP joint actuator

The graphical illustration of equivalent elastic strain is presented below.

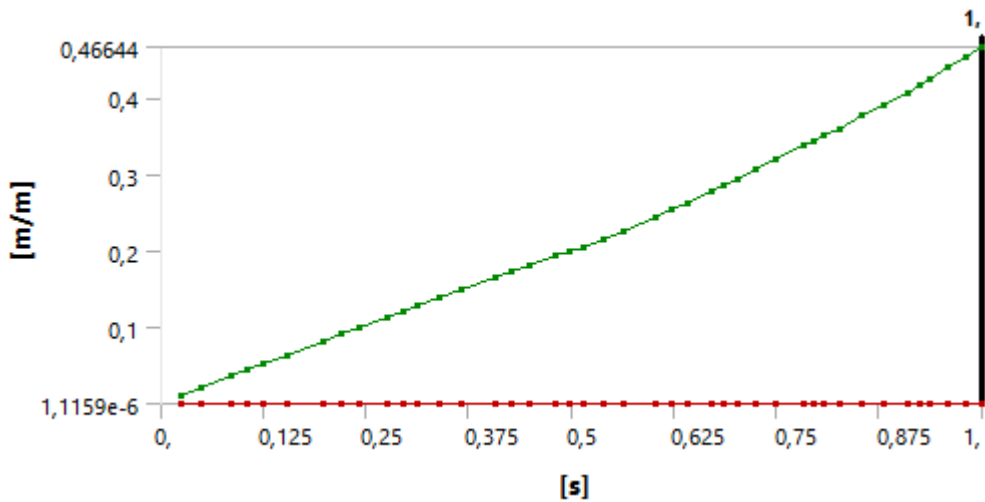


Figure 34. The graphical illustration of the equivalent elastic strain achieved by the DIP joint actuator

5 CONCLUSION

The primary aim of this master's thesis was to design a novel HE system capable of both rehabilitation and ADL purposes. For this, a pneumatic soft actuator was designed and 3D printed with silicone rubber with hardness 30 shore durometer. Similarly, the HE frame was also CAD modeled and printed with high-performance polymer PA 2200. To ensure the effectiveness of the design, a simulation of the system was modeled using ADAMS and ANSYS using finite element analysis approach. The result of simulation provided the qualitative information about the performance of the HE and the soft pneumatic actuators. On the other hand, the quantitative analysis was achieved from the review of literature and knowledge of hand biomechanics. These two approaches were significant in designing an efficient HE system.

The simulation results showed that the actuators are capable of acting bi-directionally, capable of extension and flexion. It further showed that the required displacement strain and angles can be achieved with the designed actuators. Based on this, it can be concluded that the system is adequate of delivering enough grab force for minor rehabilitation and ADL purposes. On the other hand, the use of lightweight yet strong polymer PA 2200 for HE frame and silicone actuators reduced the overall weight of the HE in comparison to the existing HEs. This, on the other hand, helped to achieve a portability functionality of the HE system.

The designed HE was very comfortable to use, to put on and to take off. Due to its modular design by the advantage of additive manufacturing, the HE achieved the objective of ensuring comfortability to the users. On the other hand, the safety of the HE was met by constraining the unnatural hand-finger movements while the use of quality and strong material reduced the risk of fatigue failure significantly as seen in the results of the simulation. This thesis accomplished the objective of the design of simple portable HE. The solution provided in the thesis was a straightforward approach.

From the qualitative and quantitative analysis, it can be concluded that the designed pneumatic actuation system HE is more effective than hydraulic systems. With the fact that

the hydraulic systems need a pressured tank and motor that are potentially difficult to carry places and noisy, the pneumatic system stands higher although two systems work on similar principle. However, on the other hand, the pneumatic systems are less accurate in comparison to electric systems. The compressibility behavior of air decrease the accuracy of the pneumatic system as this.

In summary, this thesis is capable of designing a simple and low weight pneumatic actuated HE. And for future research on this topic, the actuation of the thumb is highly preferred. The thumb biomechanics is more complicated than other fingers and thus adds the challenge for improvement of the design of the HE.

LIST OF REFERENCES

ACEO. 2017. [Referred 11.09.2017]. Available: <https://www.aceo3d.com/silicones/>

Allen-Prince, M., & Walton, J. 2011. Finger Motion Modeling for Bionic Fingers. Unpublished. July 2011.

Arata, J., Ohmoto, K., Gassert, R., Lambercy, O., Fujimoto, H., & Wada, I. 2013. A new hand exoskeleton device for rehabilitation using a three-layered sliding spring mechanism. 2013 IEEE International Conference on Robotics and Automation (ICRA). Karlsruhe, Germany. 6-10.5.2013. pp. 3902-3907.

Barr, A., & Bear-Lehman, J. 2001. Biomechanics of the wrist and hand. In: Nordin, M., & Frankel, V. J. Basic Biomechanics of the Musculoskeletal System. 3rd edn. Lippincott Williams & Wilkins. pp. 358-387.

Bebionic. 2017. The world's most lifelike bionic hand [web document]. [Referred: 23.09.2017]. Available: http://bebionic.com/the_hand

Bionics, T. 2013. How the i-limb works [web document]. [Referred: 23.09.2017]. Available: <http://www.touchbionics.com/products/how-i-limb-works>

Bundhoo, V., Haslam, E., Birch, B., & Park, E. J. 2008. A shape memory alloy-based tendon-driven actuation system for biomimetic artificial fingers, part I: design and evaluation. Robotica: Cambridge University press. pp. 1-16.

Cai, W., Meng, X. L., & Zhao, L. C. 2006. Recent development of TiNi-based shape memory alloys. Current Opinion in Solid State and Materials Science 9. pp. 296-302.

Caldwell, D.G., Medrano-Cerda, G. A., & Goodwin, M. 1995. Control of pneumatic Muscle Actuators. IEEE Control System Magazine. Vol. 2. pp. 40-48.

Carmeli, E., Patish, H. & Coleman, R. 2003. The Aging Hand. The Journals of Gerontology. The Gerontological Society of America. Series A, Volume 58, Issue 2. February 2003. pp. 146-152.

Cempini, M., Rossi, S. M. M. D., Lenzi, T., Cortese, M., Giovacchini, F., Vitiello, N., Carrozza, M. C. Kinematics and Design of a Portable and Wearable Exoskeleton for Hand Rehabilitation. 2013 IEEE International Conference on Rehabilitation Robotics. Seattle, Washington, USA. 24-26.6.2013.

Cortese, M., Cempini, M., Ribeiro, P. R. A., Soekadar, S. R., Carrozza, M. C., & Vitiello, N. 2015. A Mechatronic System for Robot-mediated Hand Telerehabilitation. IEEE/ASME Transactions on Mechatronics. Vol. 20, No. 4. August 2015. pp. 1753-1764.

Craig, J. J. 2005. Introduction to Robotics: Mechanics and Control. Third edition. Upper Saddle River, NJ 07458. Pearson Education, Inc. 2005. 408p.

Festo. 2012. ExoHand- New areas for action for man and machine. [Referred 12.09.2017]. Available: <https://www.festo.com/group/en/cms/10233.htm>

Godwin, K. M., Wasserman, J., & Ostwald, S. K. 2011. Cost Associated with Stroke: Outpatient Rehabilitative Services and Medication. Topics in Stroke Rehabilitation. Volume 18, 2011- Issue sup1: Health Services Research: Methodology, measurement, and Management. pp. 676-684.

Grebenstein, M. 2014. Approaching Human Performance: The Functionality –Driven Awiwi Robot Hand. Springer International Publishing. Switzerland. 208 p.

Heo, P., Gu, G. M., Lee, S., Rhee, K., & Kim, J. 2012. Current Hand Exoskeleton Technologies for Rehabilitation and Assistive Engineering. International Journal of Precision Engineering and Manufacturing, Vol.13, No.5. pp. 807-824.

Hiraoka, M., Nakamura, K., Arase, H., Asai, K., Kaneko, Y., John, S. W., Tagashira, K., & Omote, A. 2016. Power-efficient low-temperature woven coiled fiber actuator for wearable applications. *Nature.com: Scientific Reports*. 4.11.2016. pp. 1-9.

Hollister, A., & Giurintano, D. J. 1995. Thumb Movements, Motions and Moments. *Journal of Hand Therapy*. Vol. 8, Issue 2. April-June 1995. pp. 106-114.

In, H. K., Kang, B. B., Sin, M. K., & Cho, K. J. 2015. Exo-Glove: A Wearable Robot for the Hand with a Soft Tendon Routing System. *IEEE Robotics & Automation magazine*. March 2015. pp. 97-105.

In, H. K., Cho, K. J., Kim, K. R., & Lee, B. S. 2011. Jointless Structure and Under-Actuation Mechanism for Compact Hand Exoskeleton. 2011 IEEE International Conference on Rehabilitation Robotics. Rehab Week Zurich, ETH Zurich Science City, Switzerland, June 29- July 1, 2011.

Iqbal, J., Tsagarakis, N. G., Fiorilla, A. E., & Caldwell, D. G. 2009. Design Requirements of a Hand Exoskeleton Robotic Device. *Proceedings of the 14th IASTED International Conference. Robotics and Applications (RA 2009)*. Cambridge, MA, USA. 2-4.11.2009. pp.44-51.

Jones, L. A., & Lederman, S. J. 2006. *Human Hand Function*. Oxford University Press. 269p.

Kargov, A., Pylatuik, C., Martin, J., Schulz, S., & Döderlein, L. 2004. A comparison of the grip force distribution in natural hands and in prosthetic hands. *Disability and Rehabilitation*. *Disability and Rehabilitation*, Vol. 26, No.12. pp. 705-711.

Kotaro, T., Akai, M., Kadota, K., & Kawashima, K. 2010. Development of Grip Amplified Glove using Bi-articular Mechanism with Pneumatic Artificial Rubber Muscle. 2010 IEEE International Conference on Robotics and Automation. Anchorage Convention District, Anchorage, Alaska, USA. 3-8.5.2010. pp. 2363-2368.

Kwakkel, G., Kollen, B. J., Grond, J. V. D., & Prevo, A. J. H. 2003. Probability of Regaining Dexterity in the Flaccid Upper Limb: Impact of Severity of Paresis and Time since Onset in Acute Stroke. In *Stroke*. Volume 34. Issue 9. August 2003. pp. 2181-2186.

Lahoz, R., & Puertolas, J. A. 2004. Training and two-way shape memory in NiTi alloys: influence on thermal parameters. *Journal of Alloys and Compounds* 381. pp. 130-136.

Lauri, C., Jia, Y., Toro, M. L., Stykov, M. E., Kenyon, R. V., & Kamper, D. G. 2010. A pneumatic Glove and Immersive Virtual Reality Environment for Hand Rehabilitative Training after Stroke. *IEEE Transactions on Neural Systems and Rehabilitation Engineering*. Vol. 18, No. 5. October 2010. pp. 551-559.

Lee, J., Hwang, D., Kim, M., & Kim, K. 2016. A Feasibility Test of Underactuated Robotic Prosthetic Fingers Actuated by Shape Memory Alloy. 6th IEEE RAS/EMBS International Conference on Biomedical Robotics and Biomechanics (BioRob). UTown, Singapore. 26-29.6.2016. pp. 554-560.

Lee, K., Liu, D, Dong., Perroud, L., Chavarriga, R. & Millan, J. R. 2017. A brain-controlled exoskeleton with cascaded event-related desynchronization classifiers. *Robotics and Autonomous Systems* 90. pp. 15-23.

Lin, J., W, Y., & Huang, T.S. 2000. Modeling the Constraints of Human Hand Motion. *IEEE Proceedings Workshop on Human Motion*. Los Alamitos, CA, USA. 8-8.12.2000. pp. 121-126.

Luck, S.J. 2014. *An Introduction to the Event-Related Potential Technique*. 2nd edn. MIT Press, Cambridge, US; London. 406 p.

MA, Zhou., & Ben-Tzvi, P. 2015. RML Glove- An exoskeleton Glove Mechanism with Haptics Feedback. *IEEE/ASME Transactions on Mechatronics*. Vol.20, No.2. April 2015. pp. 641-652.

Miskelly, F. G. 2001. Assistive technology in elderly care. In: Age and Aging. Volume 30, Issue 6. 1 November 2001. pp. 455-458.

Moromugi, S., Kawakami, K., Nakamura, K., Sakamoto, T., & Ishimatsu, T. 2009. A tendon-driven glove to restore finger function for disabled. ICROS-SICE International Joint Conference 2009. Fukuoka International Congress Center, Japan. 18-21.8.2009. pp. 794-797.

National Institute of Health. 2016. World's Older Population Grows Dramatically. [Referred 12.09.2017]. Available: <https://www.nih.gov/news-events/news-releases/worlds-older-population-grows-dramatically>

Niedermeyer, E & Silva, F. L. D. 2005. Electroencephalography- Basic Principles, Clinical Applications, and Related Fields. 5th edn. Lippincott Williams & Wilkins, Philadelphia USA. 1256 p.

Polygerinos, P., Galloway, K. C., Savage, E., Herman, M., Donnell, K. O'., & Walsh, C. J. 2015. Soft Robotic Glove for Hand Rehabilitation and Task Specific Training. 2015 IEEE International Conference on Robotics and Automation (ICRA). Washington State Convention Center, Seattle, Washington. 26-30.5.2015. pp. 2913-2919.

Polygerinos, P., Lyne, S., Wang, Z., Nicolini, L. F, Mosadegh, B., Whitesides, G. M., & Walsh, C. J. 2013. Towards a Soft Pneumatic Glove for Hand Rehabilitation. 2013 IEEE/RSJ International Conference on Intelligent Robots and Systems (IROS), November 3-7, 2013. Tokyo, Japan. pp. 1512-1517.

Polygerinos, P., Wang, Z., Galloway, K.C., Wood, R. J., & Walsh, C. J. 2015. Soft robotic glove for combined assistance and at-home rehabilitation. Robotics and Autonomous Systems 73 (2015). pp. 135-143.

Rahman, M. M., Choudhary, T. T., Sidek, S. N., & Awang, A. B. 2014. Mathematical Modeling and Trajectory Planning of Hand Finger Movements. 2014 First Conference on Systems Informatics, Modelling and Simulation. pp. 43-47.

Ranganathan, V. K., Siemionow, V., Sahgal, V., & Yue, G. H. 2001. Effects of Aging on Hand Function. *Journal of the American Geriatrics Society*. Volume 49, Issue 11. November 2001. pp. 1478-1484.

Redlarski, G., Blecharz, K., Dabkowski, M., Palkowski, A., & Tojza, P. M. 2012. Comparative analysis of exoskeletal actuators. *Pomiary Automaatyka Robotyka*. pp. 133-138.

Ryu, D., Moon, K-W., Nam, H., Lee, Y., Chun, C., Kang, S., & S, J-B. 2008. Micro Hydraulic System Using Slim Artificial Muscles for a Wearable Haptic Glove. 2008 IEEE/RSJ International Conference on Intelligent Robots and Systems. Acropolis Convention Center. Nice, France. 22-26.9.2008. pp. 3028-3033.

Schadow, J. G. 2009. *The Art Student's Guide to the Bones and Muscles of the Human Body and Lessons on Foreshortening*.

Shapeways. 2017. [Referred 10.09.2017]. Available: https://www.shapeways.com/rrstatic/material_docs/mds-strongflex.pdf

Stergiopoulos, P., Fuchs, P., & Lurgeau, C. 2003. Design of a 2-Finger Hand Exoskeleton for VR Grasping Simulation. pp. 80-93.

Sun, Y., Song, Y. S., & Paik, J. Characterization of Silicone Rubber Based Soft Pneumatic Actuators. 2013 IEEE/RSJ International Conference on Intelligent Robots and Systems (IROS). Tokyo, Japan. 3-7.11.2013. pp. 4446-4453.

Thrift, A. G., Thayabarabathan, T., Howard, G., Howard, V. J., Rothwell, P. M., Feigin, V. L., Norrving, B., Donnan, G. A., & Cadilhac, D. A. 2017. Global stroke statistics. US National Library of Medicine National Institutes of Health. pp. 13-32.

Truelsen, T., Piechowski-Jozwiak, B., Bonita, R. Mathers, C., Bogousslavsky, J. & Boysen, G. 2006. Stroke incidence and prevalence in Europe: a review of available data. *European Journal of Neurology*. Volume 13. Issue 6. June 2006. pp. 581-598.

Tubiana, R., Thomine, J-M., & Mackin, E. 1998. Examination of the Hand and Wrist. 2nd edn. Martun Dunitz Ltd. The livery House, 7-9 Pratt Street, London NW1 0AE. 399 p.

Ueki, S., Kawasaki, H., Ito, S., Nishimoto, Y., Abe, M., Aoki, T., Ishigure, Y., Ojika, T., & Mouri, T. 2012. Development of Hand-Assist Robot with Multi-Degrees-of-Freedom for Rehabilitation Therapy. IEEE/ASME Transactions on Mechatronics. Vol. 17, No. 1. February, 2012. pp. 136-146.

Villoslada, A., Flores, A., Copaci, D., Blanco, D., & Moreno, L. 2014. High-displacement flexible Shape Memory Alloy actuator for soft wearable robots. Robotics and Autonomous Systems 73. pp. 91-101.

Vorvivk, L. J. 2016. Medical Encyclopedia: Tendon vs ligament. U.S. National Library of Medicine, 2016. [Referred: 12.10.2017]. Available: <https://medlineplus.gov/ency/imagepages/19089.htm>

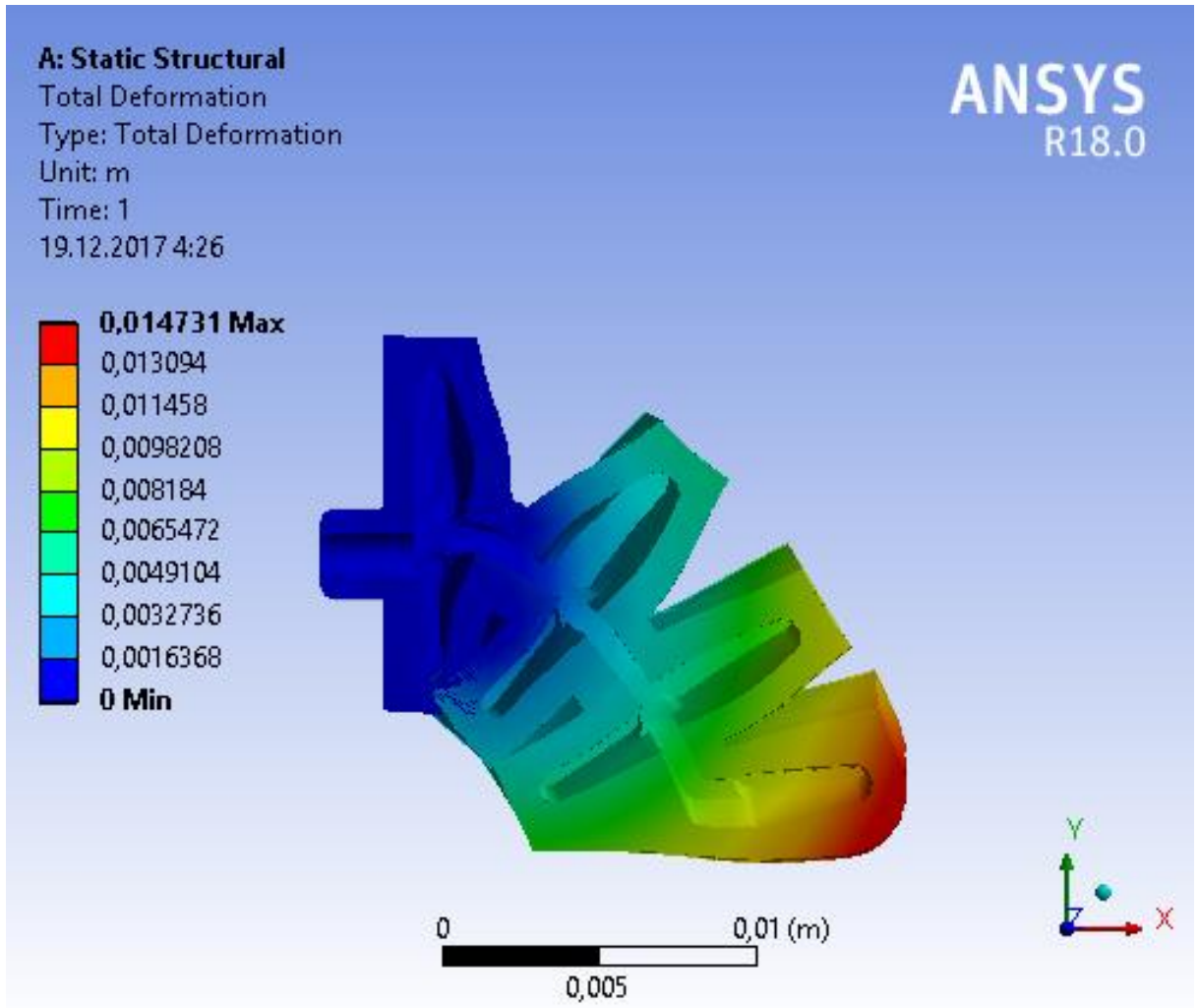
Yao, Z., Berger, C., Argubi-Wollesen, A., Weidner, R., & Wulfsberg, J. P. 2016. Highly Biometric Design of a Muscle Glove. IEEE Robotics and Automation.

Yap, H. K., Nasrallah, F., Lim, J. H., Low, F-Z., Goh, J. C. H., & Yeow, R. C. H. 2015. MRC-Glove: A fMRI Compatible Soft Robotic Glove for Hand Rehabilitation Application. 2015 IEEE International Conference on Rehabilitation Robotics (ICORR). pp. 735-740.

Zhang, F., Hua, L., Fu, Y., Chen, H., & Wang, S. 2013. Design and development of a hand exoskeleton for rehabilitation of hand injuries. Mechanism and Machine Theory 73 (2014). pp. 103-116.

Zheng, J. Z., Rosa, S. D. L., & Dollar, A. M. 2011. An Investigation of Grasp Type and Frequency in Daily Household and Machine Shop Task. 2011 IEEE International Conference on Robotics and Automation. Shanghai International Conference Center. 9-13.5.2011. Shanghai, China. pp. 4169-4175.

Total Deformation of the DIP Joint Actuator (Cross Sectional View)



Equivalent Elastic Strain of the DIP Joint Actuator (Cross Sectional View)

